NTNU
Norwegian University of
Science and Technology

Eyes beneath the surface

using a miniROV to reveal the habitat and
dietary choices of the European shag

Jørgen Strømsholm

Master of Science
Submission date: June 2018
Supervisor: Geir Johnsen, IBI
Co-supervisor: Martin Ludvigsen, IMT

Norwegian University of Science and Technology
Department of Biology

Acknowledgments

The work for this thesis took place at the Norwegian University of Science and Technology (NTNU) January to May 2018. The field data were collected during a scientific cruise to Runde in Norway in June 2017, and further analyzed at Trondhjem Biological Station (TBS) and NTNU SeaLab, at the Department of Biology.

Credit must be given where credit is due; I would hereby give an enormous "THANK YOU" to my commander in chief, my supervisor Geir Johnsen, for all the help with this thesis! You were the first, and last at NTNU, I have heard preach that it was in your best interest that the students would reach their fullest potential – because soon, the student would succeed your throne. You were very professional in your feedback, even though you always have a humorous remark or story to tell. When you pitched the idea of working with a newly and locally developed underwater drone, I was sold! You made the scientific cruise a memory I would cherish for the rest of my life, and I really hope our paths cross in the future.

I would also like to thank my co-supervisor, Martin Ludvigsen, for always helping me with the technical tenet during both the scientific cruise and the writing up this thesis. I would also like to thank my flatmate during the cruise, Signe Christensen-Dahlsgaard. You gave me exceptionally good help on the bird-ecology and with analyzing the results from the instrumented shags. I would also like to thank Roger Kvalsund and Jenny Ullgren at Runde Miljøcenter for all your help, as well as Trine Bekkby, with all the help when questions about habitat mapping in Norway need an answer. And further thank you for risking your life (in a safe manner of course) collecting pellets in the nesting colony, Lisa Graham.

I would like to give an explicit thank you to my dearest Jakob and Heidi, thank you so much for all of your praise and patience during the work on this thesis. I am really looking forward to a relaxing summer with the two of you, and to countless hours of playing and exploring the world!

Further, I would like to thank Kaja Lønne Fjærtoft, you made this special time in our lives bearable. All your wisdom, knowledge and funny remarks really made the song: "When the goings get though, the Though get going"! Furthermore, I would also like to thank all the other students at TBS and SeaLab for all the memorable laughs, and especially Guri, for handing me a beer as I am writing this. Thank you all!

Trondheim, May 2018

Jørgen Strømsholm

Frontpage: Survey footage modified by Lise Skomsvold. Shag copyrighted from Espen Rekdal @ SeaPic

Abstract

The population of sea birds in Norway is drastically declining, and numbers of breeding European shag (*Phalacrocorax aristotelis*) in the nesting colony in Runde, Norway, has declined with ~96 % in the last 40 years. Mapping and monitoring marine habitats are important for a proper marine spatial management, and governmentally funded mapping-programmes are contributing to the knowledge of the deep sea floor. However, shallow coastal habitats (sea floor and kelp forest) off the Norwegian coast, where sea birds forage, have not been mapped – leaving large knowledge-gaps. If reasons for the population-decline of sea birds is to be answered and their foraging habitat has to be protected, the knowledge of all trophic levels in the kelp forest ecology, including the prey species for shags in foraging areas, is strongly needed.

The aims of this thesis was to use enabling technology such as a small remotely operated vehicle to map kelp forest and fish species. Instrumented shags were equipped with trackers for geo-position and diving depths. Aerial drones (quadrocopter) were used to give an spatial overview of the foraging area and position of the remotely operated vehicle. The fish prey (species and sizes) for shags were analyzed using fish-otoliths (from regurgitated bird pellets). All information was put together to map the habitat and to reveal the dietary choices of European shag off the coast of Runde in Norway.

Instrumented shags revealed where, how deep and for how long time they dived (indicating a good or bad area to forage in), and showed fidelity for several distinct areas. From imagery gathered by the remotely operated vehicle in one of the areas, 56 % of all fish-observations were at the same depth as European shags dived. From collected pellets in nesting colony, otoliths revealed the species composition (20 % Labridae species, 67 % of Gadidae species and 7 % of *Ammodytes* species), and size (back-calculation) of prey the European shags foraged on. The calculated mean length of Labridae and Gadidae species was respectively 134.6 mm and 117.3 mm, while the observed mean length from imagery (including the immersion effect of 1.3) was 113.0 mm for both families of fish (however can length of observed fish not be verified as the imagery lacks a size scaling tool for size and distance).

The experimental study approach in this thesis was successful – as habitats in exposed-, sheltered-, and close to shore-areas was mapped. The usage of instrumented sea birds allowed us to follow the birds to their preferred foraging depths with technology such as remotely operated vehicle. However, the remotely operated vehicle has its drawbacks (camera and scale measuring tool to name the most pressing) for scientific work. The different mapped habitats was successfully classified using the European Nature Information System classification hierarchy – a more complex system than the Norwegian Directorate for Nature Management proposes. As most of the kelp-occurrence in coastal Norway is model-based, this survey will further argue the need for a standard with a better fit for surveys done in shallow water than the current Norwegian Standard or European Standard for habitat mapping.

Sammendrag

Sjøfugl-bestanden i Norge har falt drastisk de seneste år, hvor antall hekkende toppskarv (*Phalancrocorax aristotelis*) ved fuglekolonien på Runde har sunket med ~96 % de siste 40 årene. Kartlegging og overvåkning av marine habitat er viktig dersom Norskekysten skal forvaltes korrekt. Statlig finansierte kartleggingsprogrammer samler informasjon om havbunnen, men grunne kystnære områder (grunn havbunn og tareskog), hvor sjøfugl jakter har ikke blitt kartlagt, noe som fører til store kunnskaps-hull. Dersom man skal finne årsaker til sjøfuglers bestandsnedgang og dems jaktområder skal vernes, så må kunnskap om alle de trofiske nivåene samt økologien innad i tareskogen, inklusive byttedyrene til toppskarv, samles.

Målet med studiet var å bruke muliggjørende teknologi, som en liten fjernstyrt undervannsbåt til å kartlegge tareskogen og fiskeartene som lever i den. Instrumenterte toppskarv var utstyrt med geo-lokaliserende dybdemålere. Flyvende droner ble brukt for overblikk over jaktområdet, samt finne posisjonen til den fjernstyrte undervannsbåten. Byttene til toppskarv (art og størrelse) ble stadfestet ved hjelp av otolittene (øresten) til fisk fra de samlede gulpebollene. Informasjonen som ble samlet ble dermed brukt til å kartlegge habitatet, samt få et innblikk i dietten til toppskarv som lever på øyen Runde på norskekysten.

De instrumenterte fuglene ga et innblikk i hvor, hvor dypt og hvor lenge de dykket (dermed indikerte vanskelighetsgraden av å jakte i området), samt hvor yndet området var å jakte i. Ved hjelp av bilder samlet av den fjernstyrte undervannsbåten fra et jaktområde, viste at 56 % av all observasjon av fisk var i samme dybde som toppskarven jaktet i. Og ut i fra de samlede gulpeboller så man sammensetningen av dietten (hvor 20 % bestod av leppefisk, 67 % torskefisk, mens 7 % bestod av tobis-fisk) og størrelse (regnet tilbake fra øresteiner). Den gjennomsnittlige kalkulerte lengden av leppefisk og torskefisk var henholdsvis 134.6 mm og 117.3 mm, mens observert lengde fra bilder (inklusive nedsenkningseffekten på 1.3) var 113.0 mm for begge fiskefamiliene (selv om den observerte lengden ikke kan verifiseres siden undervannsbåten manglet måleverktøy (for mål av størrelse og distanse)).

Fremgangsmåten i dette studiet ga gode resultater, siden habitater i utsatte- og beskyttede-områder, samt områder helt inntil land ble kartlagte. Bruken av instrumenterte sjøfugler muliggjorde at man kunne følge fuglen helt fra hekkeområde til jaktområde ved hjelp av fjernstyrt undervannsbåt. Til tross for dette, så har undervannsbåten sine ulemper knyttet til seg (kamera og måleverktøy for å nevne det mest pressende) til vitenskapelig arbeid. De forskjellige kartlagte områdene ble klassifisert i henhold til Europeiske Naturinformasjonssystems klassifiserings-hierarki; et mer kompleks og detaljert system enn den forslåtte fremgangsmåten til Direktoratet for Naturforvaltning. Siden majoriteten av tareforekomsten i Norge er model-basert, vil denne avhandlingen poengtere behovet for en standard som tar hensyn til kartlegging i grunne vann, framfor den nåværende Norske Standarden for habitat kartlegging.

Abbreviations

AOP	Apparent Optical Properties
CCD	Coupled Charged Device (camera sensor)
cDOM	coloured Dissolved Organic Matter (yellow substance (gilvin, humic acids))
Chl a	Chlorophyll a (indication of phytoplankton biomass)
CMOS	Complementary Metal-Oxide-Semiconductor (camera sensor)
EMODnet	The European Marine Observation and Data network
EUNIS	European Nature Information System
EUNISclass	European Natrue Information System Habitat Classification
FoV	Field of View (viewing angle of sensor)
GPS	Global Positioning System
H'	Shannon's Diversity Index
HID	High Intensity Discharge (lamp)
indet.	Species Indeterminate
IMU	Inertial Measurement Unit (navigation)
IOP	Inherent Optical Properties
L/w	Luminous effect (Lumens/watt)
LBL	Long BaseLine
LED	Light Emitting Diode
MMH	The Marine Monitoring Handbook
NGU	Geological Survey of Norway (Norges Geologiske Undersøkelse)
OOI	Objects Of Interest
ROV	Remotely Operated Vehicle
SE	Standard Error
SST	Sea Surface Temperature
TDR	Time and Depth Recorder
TSM	Total Suspended Matter (light scattering particles)
UHI	Underwater Hyperspectral Imaging
USBL	Ultra Short BaseLine
WoRMS	World Register of Marine Species
WSU	Wireless Surface Unit

Contents

List of Figures

List of Tables

1 Introduction

The Biodiversity Convention and the Marine Strategy Framework Directive (United Nations, 1992; European Commission, 2008) states that the main goal of marine spatial management is the promotion of sustainable use of marine resources, while trying to ensure that no marine biodiversity or habitats is lost as a consequence of human activity. The International Council for the Exploration of the Sea (ICES, 2017) has in their Working Group of Marine Habitat Mapping reviewed and re-defined the term "habitat" to: "a recognizable space which can be distinguished by its abiotic characteristics and associated biological assemblage, operating at particular spatial and temporal scales". The Norwegian coastline is long and complex, with fjords and islands, resulting in the total of ~72000 km coastline (Klemsdal, 1982), making the protection of marine bio-diversity and habitats hard.

MAREANO is the Norwegian multidisciplinary seabed mapping programme, funded by the Norwegian Government, with the goal of obtaining information used as a scientific basis for regulating human activities (Buhl-Mortensen *et al.*, 2015). MAREANO is using acoustic technologies such as ship-mounted multibeam echosounders, enabling for a high spatial resolution imagery of the seafloor substrate over an extensive area, but is only suppose to map outide the 12 nautical mile zone of the Norwegian coast, and not the shallow zones (Brown *et al.*, 2011). This gives a knowledge-gap in the most shallow habitats. The knowledge-gap will make it hard for creating marine spatial plans, as they require extensive knowledge of composition and distribution of communities and the characteristics of a natural habitat in a healthy state (Stelzenmüller *et al.*, 2013).

The Norwegian sea and Arctic ocean are currently experiencing climate changes, by rapid increase in sea surface temperature (SST) (IPCC, 2013), resulting in an alteration of the physical properties of water (changes in macro- and micro-nutrients supply due to a reduced mixing (Doney, 2006), acidification and de-oxygenation (solubility of CO_2 and O_2 decreases with increased temperature (Brass *et al.*, 1982; Kroeker *et al.*, 2013)) to name a few) (Brass *et al.*, 1982; Broecker, 1991; Manahan, 2017), thus affecting the distribution and composition of the marine food-web (Walther *et al.*, 2002; Manahan, 2017; Descamps *et al.*, 2017).

This thesis are using technology (such as remotely operated vehicle and drones (biological and aerial) to map the habitat (for the most part kelp forest) and the dietary choices (different species of fish) of European shag off the coast of Runde in Norway. The different sections below will give an overview of the marine food-web, sea birds, kelp forest, fish species along the coast of Norway as well as an overview of habitat mapping using remotely operated vehicle and how optical properties of water will have a key role in habitat mapping.

1.1 Marine food-web

The marine food-web is complex, and therefore not yet fully understood. The ecological flow transfers is ~10 % of the organic carbon (biomass and food) between each trophic level (Ryther's principle of food chains) (Paine, 1966; Ryther, 1969). A simplified food-web would depict four trophic levels, i.e.: level 1 (the primary producers, phytoplankton), level 2 (the primary consumers, zooplankton), level 3 (the secondary consumers, with species such as cod (*Gadus morhua*, Linnaeus, 1758), saithe (*Pollachius virens*, Linnaeus, 1758) and sand lances (*Ammodytes* spp., (Linnaeus, 1758), see definition in **Section 1.4**) and level 4 (the apex predators (fish consumers)) (Hairston *et al.*, 1960; Ryther, 1969; Pimm and Lawton, 1977; McLusky and Sargent, 1990; Rice, 1995; Edwards and Richardson, 2004).

An increase in SST will affect the complexity of the marine food-web with alterations in the quality, abundance, size and especially the relative timing of prey's arrival for the higher trophic levels (Cushing, 1982, 1990; Burgess *et al.*, 2018; Keogan *et al.*, 2018). Consequently leading to an imbalance of the well-established pattern within the food-web, described as the match-mismatch hypothesis (Durant *et al.*, 2005, 2007; Cury *et al.*, 2011).

1.2 Sea birds

Sea birds are apex predator and thus dependent on lower trophic levels sustaining a high production of fish as food source for adult birds and their chicks during the breeding season. The match-mismatch hypothesis predicts that: the recruitment of predators (here: birds) will be high if the peak of preys (here: fish) availability match the period of the highest energy-demand for predators breeding phenology; while a mismatch will ultimately lead to a poor recruitment (Durant *et al.*, 2005; Keogan *et al.*, 2018), thus, a failure of the predators yearly brood might occur – resulting in a declining population size (Durant *et al.*, 2004).

The population size of the European shag (*Phalacrocorax aristotelis*, hereafter shag), a near-shore-foraging (mainly kelp forest) and pursuit-diving sea bird (Cramp and Perrins, 1983) has for the last 40 years fluctuated (Røv, 1984). In the 1970s, shags had a roughly estimated population size of 28,000 pairs; which amounted to 35 % of the total NE Atlantic population at that time (Anker-Nilssen *et al.*, 2000; Fauchald *et al.*, 2015). At Runde, Norway, there has been registered a decrease of ~96 % in breeding pairs since 1975 - from 5000 (Barrett *et al.*, 2006; Lorentsen, 2005) to no more than 200 breeding pairs in breeding season of 2017 (Christensen-Dalsgaard, S 2018, personal communication, 15th of May). Shag shows a high flexibility in their dietary choices (Barrett *et al.*, 2007), with Norwegian bound shag foraging primarily on saithe (Lorentsen *et al.*, 2015), sand lances (Barrett and Furness, 1990) and cods (Barrett *et al.*, 1990) primarily in the kelp forest close to the nesting colony (Christensen-Dalsgaard *et al.*, 2017).

1.3 Kelp forests

Macroalgal clusters such as kelp forests are highly productive and important as predator refuge, nursery and feeding grounds for many species (Kain, 1971; Keats *et al.*, 1987). The kelp specie *Laminaria hyperborea* (Gunnerus, 1884) is by far the most dominant of throughout the Norwegian coast (Norderhaug *et al.*, 2005). As *L. hyperborea* is thriving in the coastal waters of Norway, is the distribution of other species of kelp, such as *Saccharina latissima* (Linnaeus, 1753) in a steady decline. The cause of the decline may be increased SST and macro-nutrients (particulate of organic matter) in a combination of less available micro-nutrients (Gundersen *et al.*, 2014). The kelp forest supports a diverse biodiversity, and were found to have an average density of 8000 mobile macrofauna individuals per kelp, with amphipodes and gastropodes as the most abundant groups (Christie *et al.*, 2003) and further providing habitat for several fish species (Norderhaug *et al.*, 2005).

1.4 Fish

Norderhaug *et al.* (2005) found in a well developed *L. hyperborea* forest in Finnøy, Norway, that the most abundant fish species of Gadidae (Rafinesque, 1810), was juvenile saithe, and the second most were bigger cod - species hereafter grouped to "gadoid". Also species of Labridae (Cuvier, 1816), such as goldsinny wrasse (*Ctenolabrus rupestris* (Linnaeus, 1758)) and corkwing wrasse (*Symphodus melops* (Linnaeus, 1758)) - species hereafter grouped to "labrid", finds the kelp forests as suitable habitats (Fjøsne and Gjøsæter, 1996; Steneck *et al.*, 2002). Catches of fish within the kelp forest done in a study by Norderhaug *et al.* (2005) were larger at night than during the daytime. The catches' stomach content was analyzed to be of pelagic copepods and kelp forest invertebrates (*Rissoa parva, Lacuna vincta* and *Jassa falcata* (WoRMS, 2018)) - suggesting that fish, as a visual predator, hunts for copepods diurnal and mobile epifauna nocturnally, thus utilizing the whole vertically of the forest (kelp canopy, as well as in-between the stipes and haptera) (Christie *et al.*, 2003; Norderhaug *et al.*, 2005).

As previously mentioned, is sand lances (*Ammodytes* spp. (Linnaeus, 1758), consisting of species which are not differentiated in either manangement nor estimation of population: *Ammodytes tobianus* (Linnaeus, 1758), *Hyperoplus lanceolatus* (Le Sauvage, 1824) and the *Ammodytes marinus* (Raitt, 1934)) an important prey for apex predators. The adult sand lances burrows in the sand substrate at periods of low light intensity (night and winter), while leaving their bottom hides and form large shoals during periods with high light intensity and strong tidal currents, where they prey on energy-rich copepods (Muus *et al.*, 1999).

1.4.1 Otoliths

Otoliths are two calcium carbonate-structures with both an auditory and vestibular role in vertebrates, and every species of fish have been found to have their unique shape of otoliths (Popper and Fay, 1993). Lee (1920) purposed a hypothesis that the growth incre-

ment of the fish-scale is, on the average, a constant proportion of the growth increment of the fish. On the basis of the Lee hypothesis; a correlation between the fishes individual somatic growth history and the otolith growth increment have been found (Neilson and Geen, 1982; Mosegaard *et al.*, 1988; Campana and Thorrold, 2001; Campana, 2001), and the Fraser-Lee-method is the most common and well-known back-calculation method (Francis, 1990). The hypothesis is very general, and surveys done in coastal waters in Norway (Härkönen, 1986; Jobling and Breiby, 1986; Hillersøy and Lorentsen, 2012) have found formulas which take regional variations into consideration, and fit better than the back-calculation method proposed by Lee.

1.5 Habitat mapping

With the increased governmental focus on protection of marine biodiversity and habitats, the integration of geographical-, environmental- and behavioural-data for the use in coastal zone management and planning has had an growing interest (Bekkby *et al.*, 2009). As the vastness of the Norwegian coastline makes habitat mapping hard, Bekkby *et al.* (2002) presents a model-based geo-referenced map (with the spatial resolution of 1 km^2) predicting the distribution of e.g. *L. hyperborea* along the coast of Norway by taking the bathymetry, terrain variation, light-intensity (i.e. irradiance), wave-exposure and wind conditions into consideration (while also probing stations with underwater cameras for quality control). However, habitat mapping of the Norwegian coast has proven hard due to the dynamic reality of nature and anthropogenic interactions (e.g. in northern Norway where the *L. hyperborea* have been grazed down by the green sea urchin (*Strongylocentrotus droebachiensis*, Müller, 1776) for the past 30 years (Skadsheim *et al.*, 1995), while *L. hyperborea* have been harvested in the southern- and western Norway for alginate-production since the 1970s (Jensen, 1998)). Therefore, must static maps like Bekkby *et al.* (2002) presents, never replace surveys with a much higher spatial resolution (down to 1 cm per pixel) (Bekkby *et al.*, 2013; Johnsen *et al.*, 2016), and also showing the need for monitoring the habitats (i.e. time series).

Many countries have their own standard for habitat mapping to follow, e.g. Norway follows the Norwegian and European Standard NS-EN 16260:2012 “Water quality – visual seabed surveys using remotely operated vehicles and/or towed observation gear for collection of environmental data”. The standard gives guidance on sampling strategies, geo-positioning, taxonomic identification and quantification and determining the seabed substrates and/or organisms living on or above the seabed. Although the standard is an European Standard, most of the information are scattered, fragmented or limited to a few studies which classifies habitat differently. A precursor which aims to develop consistent habitat classification through a six level classification hierarchy (an example of four of the six levels can be seen in **Figure 1.5.1**) is EUNIS (European Nature Information System (Davies *et al.*, 2004)). EMODnet (European Marine Observation and Data network (Calewaert *et al.*, 2016)), a network of organizations supported by the integrated maritime policies within the European Union,

aims to gather the European marine data of bathymetry, seabed habitats (EUNIS classified), geology, chemistry, biology, physics and human activity in one database. EMODnet has the philosophy of "collect once and use many times", which should benefit every policy makers, scientists, industry and the public.

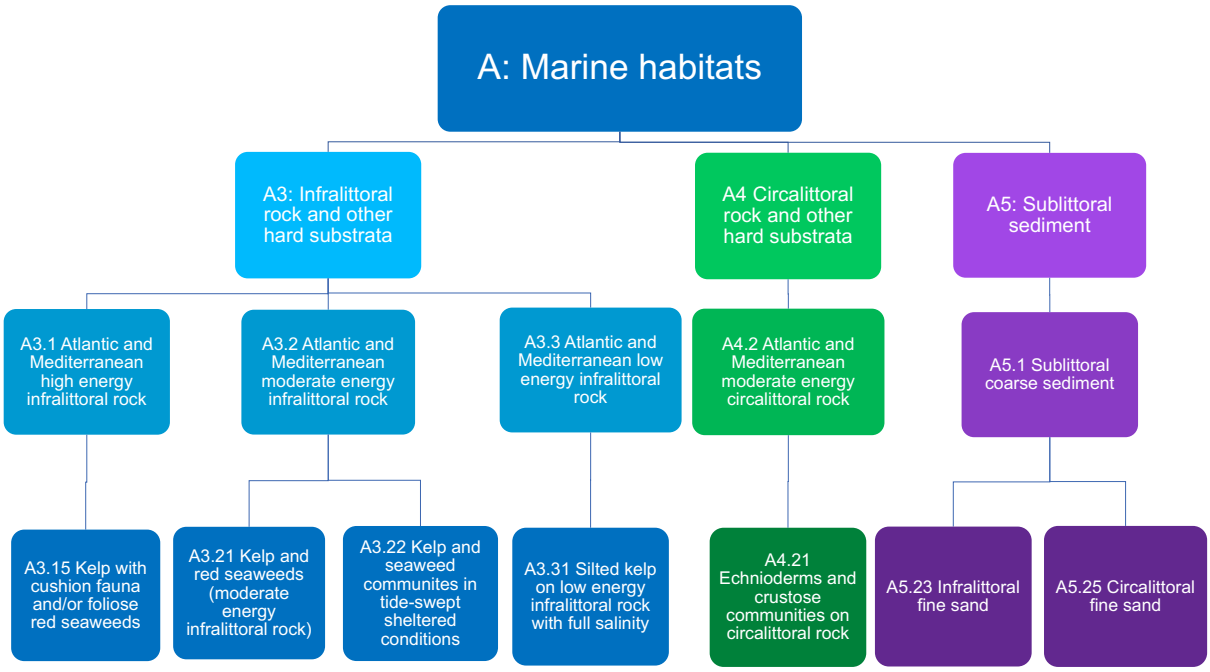

Figure 1.5.1: The first four levels of EUNIS habitat classification hierarchy (Davies *et al.*, 2004) showing potential habitats in Norwegian coastal waters, where they are defining the substrate and its characteristics, depth/light and exposure. This survey will however not explore further than level 4.

A common ecological sampling method is "line transects", which is used for illustrating a particular linear pattern or particular gradient along a community change, thus providing a visualization of change that takes place along the line, gathering information of what species or substrate is present, thus a good method for habitat mapping (Loya, 1978; Borcard *et al.*, 2004).

1.6 Remotely Operated Vehicle

Remotely Operated Vehicle (ROV) is a non-invasive mobile underwater platform tethered to the surface with an umbilical cord, enabling two-ways communication (feed of power from the mother-vessel and feed of information from the deep to the surface) (Johnsen *et al.*, 2013). The pros with a ROV is the high maneuverability (movement in three dimensions (roll, pitch and yaw-axis (x,y,z))) and, as an instrument-carrying platform, bring instruments down to far greater depths than conventional scuba-divers can explore, while the main con is the dependability of a mother-vessel that feeds ROV with power (Ludvigsen, 2010; Ludvigsen *et al.*, 2014).

A miniROV is a small, light and nimble ROV which can be deployed from either shore or a small boat, enabling it to explore more exposed and shallower sites that larger ROVs can not explore (further described in **Section 2.2.3**). It has the same capabilities as a larger

instrument-carrying platform and delivers imagery to the surface, however, miniROVs are naturally limited by size and power.

1.7 Optical properties of water

The imagery from ROVs are influenced by the optical properties of seawater and how the constituents are attenuating light (Johnsen *et al.*, 2013; Sakshaug *et al.*, 2009). Optical properties are categorized as apparent optical properties (AOPs) and inherent optical properties (IOPs), where AOPs are defined as the optical properties of the medium (water) in context with the geometrical structures of the ambient light field generated by the sun (Preisendorfer, 1976; Johnsen *et al.*, 2013). While IOPs are the optical properties of the medium regardless of the ambient light field generated by the sun (Preisendorfer, 1976), and includes the various concentrations of phytoplankton (Chl a), colored dissolved organic matter (cDOM) and total suspended matter (TSM). These IOPs will alter the sharpness, colors and contrast of objects in a given imagery due to absorption and/or scattering and/or back-scattering of light (Smith and Baker, 1981; IOCCG, 2000; Johnsen *et al.*, 2009).

1.8 Experimental aims

The aim of this study was to use a miniROV to reveal and map the habitat (sea floor and kelp forest) and dietary choices (several fish species) of European shag off the coast of Runde in Norway, using underwater video as an aid to identify objects of interest (OOI, in this case fish). The information of habitats were gathered using a miniROV deriving from AMOS (the Centre of Autonomous Marine Operations and Systems) at NTNU. Shags were instrumented with GPS (Global positioning system) and TDR (Time-Depth-Recorders) and used as biological drones to map their foraging pattern, and dietary choices (prey abundance/size and species) through the collection and analysis of regurgitated pellets.

2 Materials and methods

2.1 Study area

Data were gathered during a scientific cruise onboard the NTNU-owned research vessel (RV) Gunnerus to the island Runde (62°24'01.9"N 5°37'27.0"E), Møre og Romsdal, Norway (**Figure 2.1.1**), from 17-27th of June 2017. Runde is situated in Herøy municipality in Søre Sunnmøre and is one of the southern most nesting colony hosting species as Atlantic puffin (*Fratercula arctica*, (Linnaeus, 1758)), Black-legged kittiwake (*Rissa tridactyla*, (Linnaeus, 1758)), Northern Gannet (*Morus bassanus*, (Linnaeus, 1758)) and Northern Fulmar (*Fulmarus glacialis* (Linnaeus, 1761)), as well as the shag. The main site for nesting is the hillside of Kaldekloven and Storholet (Runde Miljøsenter, 2018).

The weather conditions during the cruise can be seen in **Table 2.1.1**. The first three days had southwesterly near gale winds and high precipitation, giving unfavourable conditions for the miniROV. Those days were used to master the maneuverability, techniques with release and retraction of umbilical cord and storage of footage, within the sheltered harbour of Runde molo. The latter days the weather calmed and gave favourable conditions to be offshore with an open work boat, "Polarcirkel" and the "Lophelia research and transport vessel".

Table 2.1.1: Weather information, from Svinøy weather station (station #59800) (Yr.no). Wave-data, from a *in situ*-buoy outside the neighbouring island Godøya (Norwegian Public Roads Administration).

Date	Temperature	Wind	Significant waveheight	Max waveheight	Wave direction
	(°C)	(m/s)	(m)	(m)	(°)
June 17th 2017	12.7	12.0	0.8	1.2	277.7
June 18th 2017	11.7	15.6	1.3	1.9	275.7
June 19th 2017	11.7	13.1	1.5	2.2	282.8
June 20th 2017	9.8	10.7	1.8	2.9	294.0
June 21st 2017	9.8	4.9	1.3	2.0	302.5
June 22nd 2017	11.4	3.4	0.6	1.0	302.9
June 23rd 2017	11.3	5.4	0.7	1.1	291.0
June 24th 2017	11.3	9.2	1.3	1.9	284.2

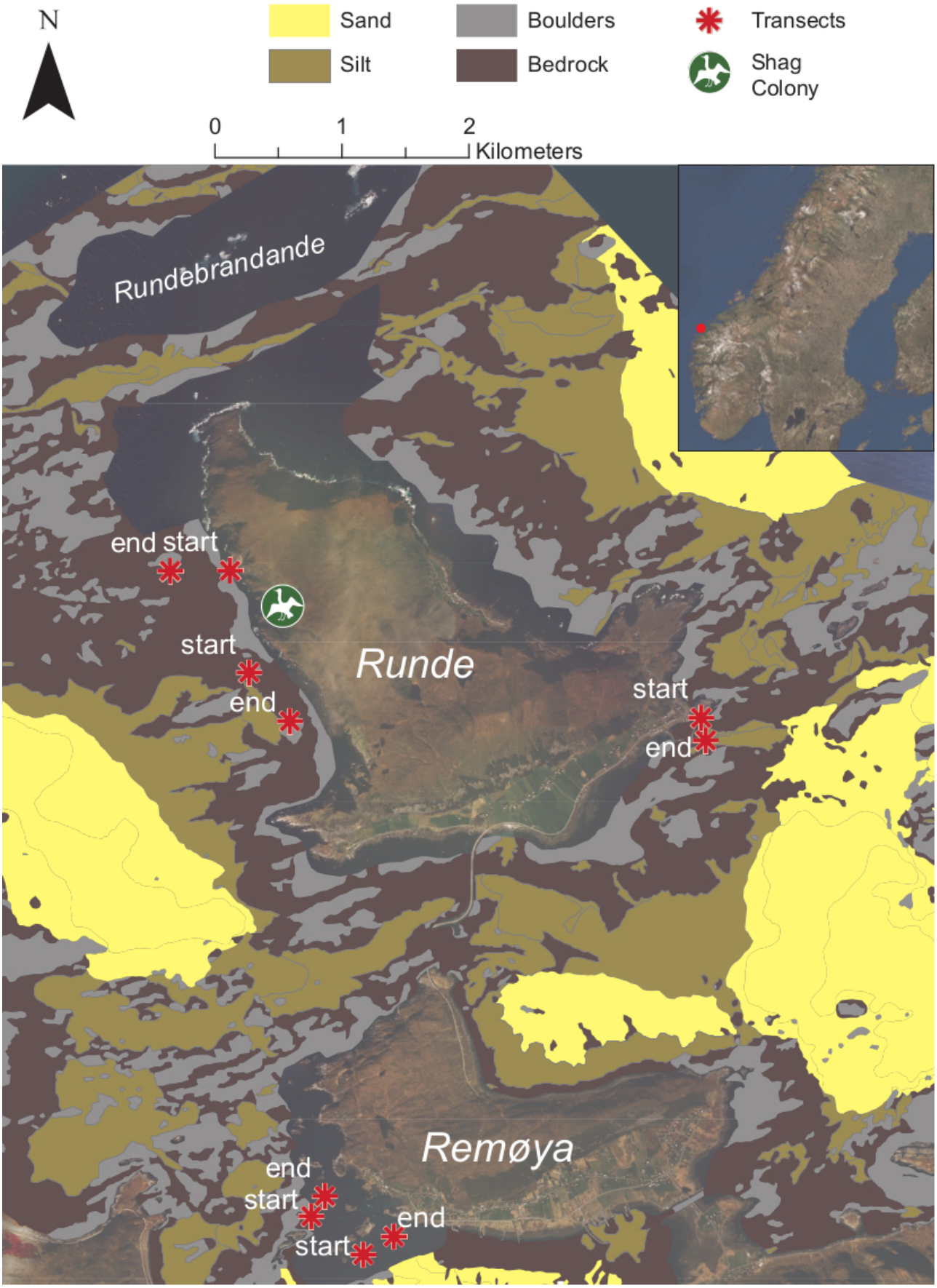

Figure 2.1.1: Bottom substrate map at Runde and Remøya, Norway with N25-detailed sediment-map (1:5000) from Geological Survey of Norway (NGU) surrounding the island. Note that the overlayed sediment-map covers the shoreline unevenly, and not all transects are covered by the map. The green bird on the north-west coast of Runde indicates the area for the shags' nesting colony.

2.1.1 Habitat description

The sea floor around Runde and Remøya comprises shallow areas dominated by bedrock, sand and silt. Bedrock is the major substrate for the kelp forest providing feeding habitat for European shag. The sediment-map from NGU (Geological Survey of Norway, 2018) is overlaid a satellite photo of Runde and the neighbouring island Remøya (**Figure 2.1.1**). The surrounding substrate of both islands are comprised of bed rock, pebbles (in different sizes), silt and sand. In areas with hard substrate the predictions of kelp-occurrence in the shallowest parts (<20 m) are high (Bekkby *et al.*, 2002). There are large sandbanks off the coasts of both islands. These habitats make the surrounding waters off both islands suitable for species such as gadoids (Godø *et al.*, 1989; Salvanes *et al.*, 1994), labrids (Skiftesvik *et al.*, 2014) and sand lances (Holland *et al.*, 2005); thus making the waters a good foraging area for sea birds (Barrett *et al.*, 2007).

2.2 Drone platforms

2.2.1 Biological drones (European shag)

Shags were captured from randomly selected nests in Kaldekloven nesting colony to even out the sex distribution within the sample of birds, and instrumented with either GPS-loggers (i-gotU GT-120, Mobile Action Technology, Taiwan) or with a combination of GPS- and Time Depth Recorder (TDR) loggers (G5, CEFAS Technology, UK) to 3-4 middle tail feathers. The maximum weight of the sensors were 30.6 g (1.6 and 1.8 % of mean body weight for males and females). The TDR-loggers recorded the diving behavior and were configured to record temperature and pressure every second, while the GPS position recorded every 30 seconds (following Christensen-Dalsgaard *et al.* (2017)). During the instrumentation of shags, their regurgitate pellets of indigestible matter (otoliths, thick parts of gastropod shells and mouth-pieces from polychaetes) were collected in the nesting colony. These regurgitated pellets were further used to identify fish species and age (size).

2.2.2 Aerial drones (Quadrocopters)

A quadrocopter drone (1.4kg) Phantom 4 Advanced (Dji, China) was used for aerial footage during the survey. It was equipped with a videocamera, with a 4Kp60 1" Complementary Metal-Oxide-Semiconductor (CMOS) sensor with a 20 MP [†]. An Inspire 1 (Dji, China) (3kg) equipped with a 12.4 MP 4Kp25 1/2.3" CMOS camera, was used to find the miniROV during transect #3 [††].

[†] Operated by Lisa Graham (NTNU).

[††] The drone was supplied and operated by Maritime Robotics's Torbjørn Houge.

2.2.3 Underwater drone (miniROV)

The front of the miniROV comprises of a camera (sensor-specifics in **Table 2.2.1**) and 10 white Light Emitting Diodes (LED) search-lights (specified to 2000 lumen). The 8 kg miniROV has a hull design which is hydrodynamic and hydro-balanced for stability and performance in diverse ocean conditions, and is pressure rated to a depth of 150 m. Three thrusters (3 x 350 W, 2 rear and 1 vertical center) gives a theoretically max speed of 2 ms^{-1}.

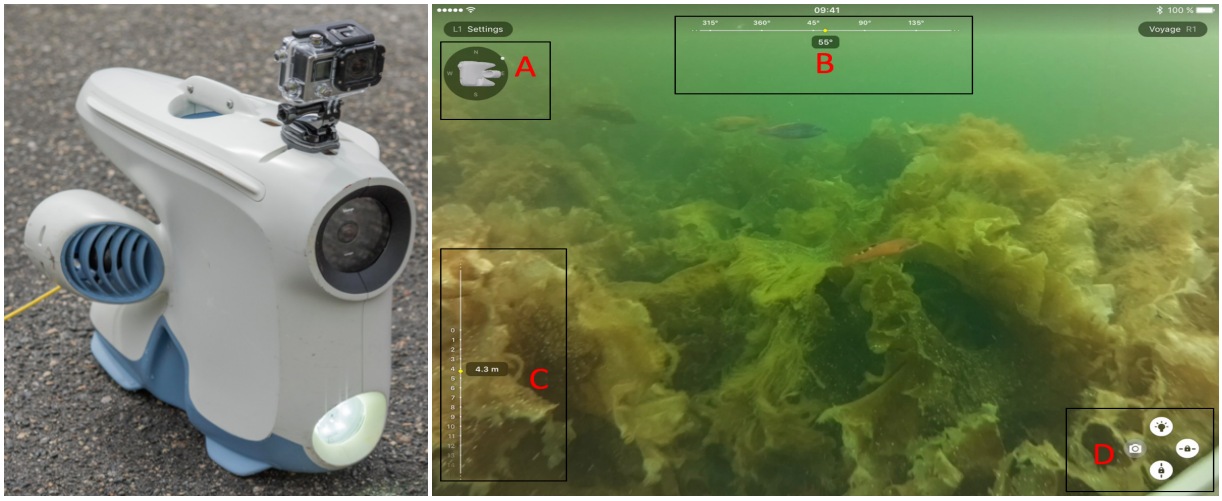

(a) **(b)**

Figure 2.2.1: (a) the miniROV BluEye (BluEye.no, 2018), with the detachable GoPro Hero 4 Silver (GoPro, USA). **(b)** the interface within the BluEye iOS app giving a live feed from the miniROV, which was controlled with a SteelSeries Nimbus (Denmark). **A**: the compass rose, with the indicated direction as well as the spatial orientation of the miniROV in relation to the operator. **B**: the linear compass and heading of the miniROV. **C**: the current depth of the miniROV and **D**: the controls for toggling search lights (2 steps), snapshot (frame-grab saved within the app) and for horizontally and vertically locking the miniROV.

The miniROV was equipped with an Inertial Measurement Unit (IMU) providing movement data in 3 dimensions by the use of a with 3-axis gyro and 3-axis accelerometer, depth sensor, magnetometer (compass) and inside and outside temperature sensor). These sensors allow for two modes of automation to be operated; auto-heading (horizontal-locking) and auto-depth (vertical-locking) (BluEye.no, 2018).

The miniROV was tethered to the surface through an umbilical cord, which is a 5 mm cobber-wire with positive buoyancy, with a data bandwidth of ~100 MBps, enabling two-way communication (video- and signal-feed to the surface and commands down to the miniROV). The miniROV used in this survey was equipped with a 75 m long umbilical, attached topside to a Wireless Surface Unit (WSU) for further wireless connection to smart-phones or tablets as well as a wireless controller (the SteelSeries Nimbus (Denmark)).

The wireless signals go through a BluEye app (iOS/Android), and are displayed as seen in **Figure 2.2.1b**. It feeds the pilot information about the depth, compass heading and spatial position orientation, and the opportunity to toggle the search lights, locking of automation and a snapshot (BluEye.no, 2018).

During the survey, the miniROV was equipped with a detachable GoPro Hero 4 Silver (the specifics in **Table 2.2.1**) capturing footage in Wide Field of View (FoV).

Table 2.2.1: Camera sensor specifications for both cameras used.

	BluEye	**GoPro Hero4 Silver**
Weight	3 g	-
Video modes	1080p30, 720p60 and 640x480p60&90fps	4K15, 2.7K30, 1080p60, 720p120 and 480p240
Sensor	Coupled Charged Device (CCD)	Complementary Metal-Oxide-Semiconductor (CMOS)
Sensor resolution	3280 x 2464 pixels	3840 x 2160 pixels
Sensor image area	3.68 x 2.76 mm	5.37 x 4.04 mm
Megapixel per image	8	12
Rate of transfer	16 Mbps	30 Mbps
Pixel size	1.12 x 1.12 μm	1.55 x 1.55 μm
Optical size	1/4" / 6.35 mm	1/2.3" / 11.04 mm
Focal length / Underwater	3.04 mm / 4.12 mm	2.92 mm* / 3.94 mm
Horizontal FoV (air)	62.2°	122.6°
Vertical FoV (air)	48.8°	94.4°
Focal ratio (f-stops)	2.0	2.8

* equivalent to 35 mm in GoPro-mode: Wide view (17.2 mm), Medium view (21.9 mm) and Narrow view (34.4 mm)

2.3 ROV-transects

To illustrate gradients patterns and to survey of species community change, a series of line transects were conducted in the waters outside Runde and Remøya (for transects see **Figure 2.3.1** and information in **Table 2.3.1**).

Table 2.3.1: GPS positions for the start and end-position, length, range of depth and habitat type to the five transects. Length denotes distance from start to end of each transect.

Transect	Start	Stop	Length	Depth
#1 - Kaldekloven	62°24'144"N 5°35'235"E	62°24'119"N 5°34'511"E	470 m	0 - 33 m
#2 - Handfangansvika	62°23'494"N 5°35'416"E	62°23'387"N 5°36'745"E	500 m	0 - 40 m
#3 - Runde molo	62°23'519"N 5°39'519"E	62°23'550"N 5°39' 490"E	100 m	0 - 23 m
#4 - Remøya-1	62°21'345"N 5°36'585"E	62°21'409"N 5°37'426"E	190 m	0 - 25 m
#5 - Remøya-2	62°21'278"N 5°37'293"E	62°21' 334"N 5°37'446"E	280 m	0 - 27 m

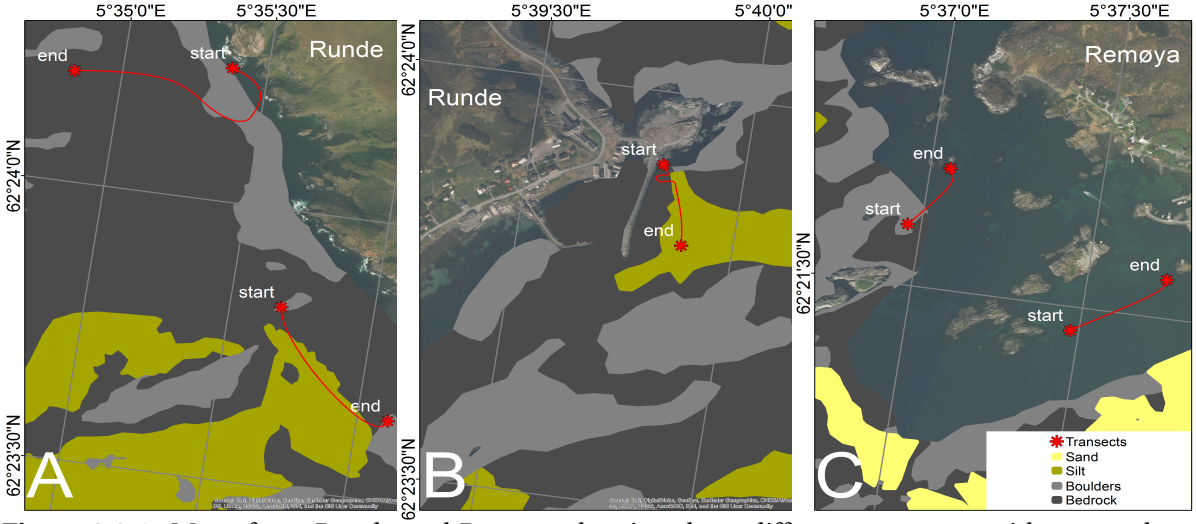

Figure 2.3.1: Maps from Runde and Remøya showing the 5 different transects, with an overlay of N25-detailed sediment-map which gives a prediction of kelp occurrence. The red asterisk gives the position of each transect and an estimation of the route for the miniROV. The upper transect in **A** is transect #1 and the lower transect #2, while transect #3 off the Runde molo can be seen in **B**. Note that the sediment-map does not cover transect #4 and #5 in **C**.

Transect #1 was done just west of the hillside of Kaldekloven, the nesting site for most sea birds on the island. Transect #2 was conducted over a sand substrate between Stakkeneset and Måganeset, a historic fishing ground for sand lances. Transect #3 was done east of the Runde molo. The transect was done in three parts, where the first part was a pre-survey of bathymetry. At the end of the umbilical the miniROV then surfaced, and an aerial drone was used to get fixed GPS-position of the miniROV. The second part commenced by the miniROV diving to the seafloor and following it towards the shore. The third part consisted of deploying the miniROV from a work boat and finishing the outer and latter part of the transect. Transects #4 and #5 were done in a sheltered area on the east-coast of neighbouring island of Remøya.

2.4 Data-analysis

2.4.1 Instrumented birds

Following Christensen-Dalsgaard *et al.* (2017), the GPS-position were coupled with data from the TDR-loggers. The spatial position of shag dives were determined by relating the dives to the GPS-position closest in time, restricted to a maximum of 30 second difference between the GPS-position, and start or end of dive (to compensate for there being no GPS position acquisition while birds were submerged in the dives). In further processing of logger data, dives within 300 m of the nesting colony (not regarded as foraging trips), shallower than 1.5 m (regarded as washing dives) and speed ≥3 ms^{-1} (deemed unlikely) were excluded from the dataset (Christensen-Dalsgaard *et al.*, 2017).

2.4.2 Underwater imagery from miniROV

Imagery from the miniROV were transferred from the WSU to an iPAD 4 (Apple Inc., USA), sharing monitoring screens with a MacBook Air (Apple Inc., USA), where the live feed was recorded as video in MOV-format, with a spatial resolution of 1600x1200 pixels; and hereafter called "BluEye footage". The imagery from the GoPro was in MP4-format, with a spatial resolution of 1920x1080 pixels (1080p HD), hereafter "GoPro footage". The BluEye footage was scaled and more compressed than the GoPro footage, influencing the spatial resolution, overall quality and size of the images.

2.4.3 Video analysis

BluEye footage were opened in ImageGrab software (Glagla, 2017), which created a frame-grab every 5 seconds. Each frame-grab was analyzed and information of the depth and number of biological objects of interest (OOI) was noted. Every frame-grab was treated uniquely, meaning that fish too blurry to distinguished was discarded, regardless if the fish could be identified on the past frame-grab. Fish with recognizable characteristics of gadoids or labrids, but could not be identified to species, was categorized as Gadidae indeterminate (hereafter indet. as explained in (Sigovini *et al.*, 2016)) or Labridae indet. (<10 cm due to the size of fish made it hard to determining the species). Identified gadoids was categorized into sizes of <10 cm, 10-20 cm and >20 cm, while identified labrids was categorized into <10 cm and >10 cm. There were no cuckoo wrasse >10 cm sightings; therefore, categorized as only <10 cm.

The analysis was manual and took between three to four hours per transect to finalize, all depending both on the length of the transect and the variation in observable life in each frame-grab. The information noted from the video-analysis is presented in **Figures 3.4.1**, **3.4.2**, **3.4.3**, **3.4.4** and **3.4.5**.

2.5 Statistical and numerical methods

2.5.1 Otolith measurement from shag pellets

Collected shag regurgitated pellets[†] containing undigested otoliths from fish were measured, analyzed and then sorted by the different species[††] (Hillersøy and Lorentsen, 2012), revealing fish species and biomass in shag diet. Under normal conditions, there will be an almost perfect symmetry between otolith-pairs (Vignon and Morat, 2010), thus excluding duplicates in further processing of data. The mean fish length was back-calculated by the mean otolith-length using equations as shown in Härkönen (1986). However, otoliths too small for species identification other than Gadidae indet. (<3 mm) were considered as saithe 0-group (<1 year) and the fish length was back-calculated using equations as shown in Jobling and Breiby (1986), thus accounting for regional variations in the species size (Hillersøy and Lorentsen, 2012).

2.5.2 Shannon's diversity index

The Shannon's Diversity Index (H') was used as a statistical description of the biodiversity in the transects done in Runde. To avoid further confusion with naming the index as seen in Spellerberg and Fedor (2003), this thesis will use the name Shannon's Diversity Index (H'). H' measures the amount of information needed for every member of a community to be described, and if p_i is the proportion of individuals of species i, then the diversity (H') is: (Shannon and Weaver, 1949):

$$H' = -\sum_{i=1}^{s} P_i \, log \, p_i \tag{2.5.2.1}$$

where s is the number of species, and $p_i = n_i / N$ for the ith species (Valiela, 1984). The value of H' usually ranges from 1.5 to 3.5 (Jost, 2006). H' is dependent on an assumption that the sample used is a random sample of the community and thus a useful measure since the evenness can be calculated using it. Evenness (E) is the ratio of the actual H' value to the maximum value; thus ranging from 0 to 1 (Hill, 1973):

$$E = \frac{H'}{H_{max}} \tag{2.5.2.2}$$

[†] Collected, max one day old, pellets by Signe Christensen-Dalsgaard (NINA) and Lisa Graham (NTNU)
[††] Work done by Grethe Hillersøy (NINA)

When E = 0, either no or only one species is present - indicating no biodiversity. Equitability were measured using the scale (0-1) defined by Jakobsen (2016):

E = 0	not present
E = 0.1 – 0.3	low diversity
E = 0.3 – 0.5	medium diversity
E = 0.5 – 0.9	high diversity
E = 1	“perfect” diversity/evenness

2.6 Data processing

Visualization of geo-position data from instrumented shags and producing maps was done in ArcGIS (Esri, USA). Observations from the frame-grabs and otolith-data were noted and calculated, and figures were produced in Microsoft Excel 2016 (Microsoft Corp., USA). And adjustments and labelling of figures and frame-grabs where conducted in Microsoft PowerPoint 2016 (Microsoft Corp., USA) and further exported in the PDF-format for good scalable figures.

3 Results

3.1 GPS- and TDR-data from instrumented shags

The mean depth of diving shags were 25 m. Of recorded GPS-positions (n = 861), 0.02 % were outside the nesting colony (see the green bird in **Figure 3.1.1**) - the area where transects #1 and #2 were conducted and 0 % in the area where transect #3 was conducted and 0.06 % of dives in area where transects #4 and #5 were conducted. Information from retrieved loggers (n = 7), of instrumented shags can be seen in **Figure 3.1.1**, revealing the areas where the shags dived. This information was used to decide where transects #4 and #5 could be conducted.

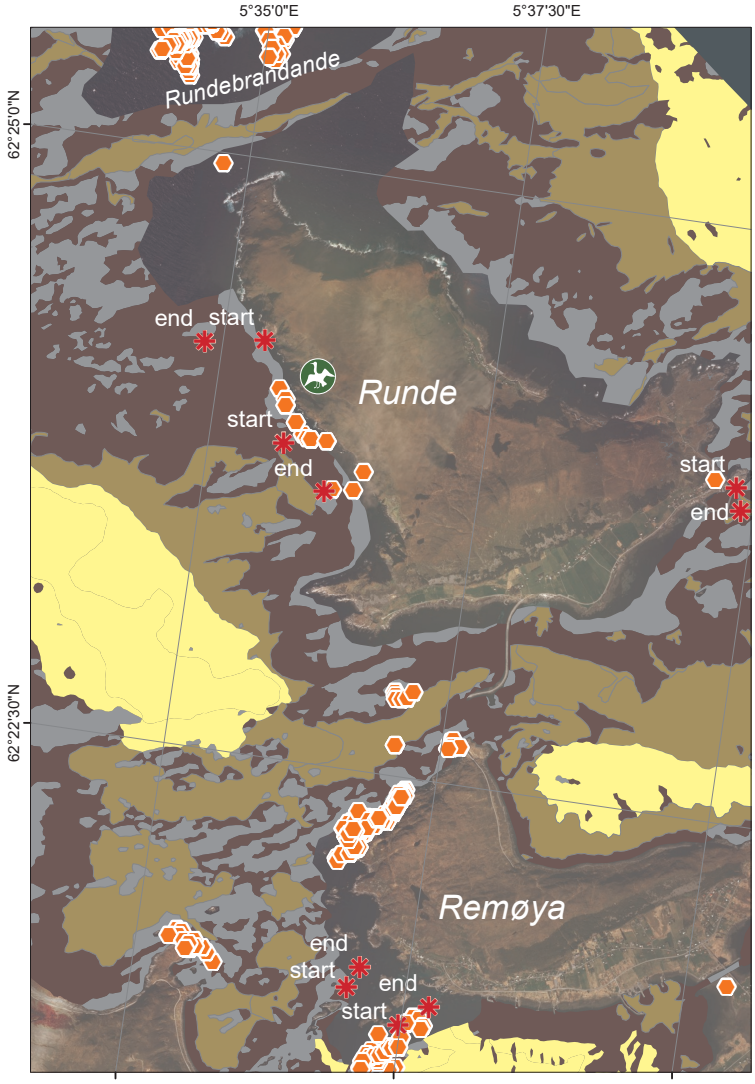

Figure 3.1.1: GPS positions (n = 861) from loggers (orange spots) shows areas of recorded shag dives. The green bird on the north-west coast of Runde indicates the area for the shags' nesting colony. Note that the majority of dives recorded are within an area not covered by the sediment-map north of Runde ("Rundebrandane" (62°25'32.8"N 5°34'46.2"E)) and an area north-west of Remøya. The red asterisks are transects.

3.2 Encountered fish taxa

Table 3.2.1 lists all the families and species (with author-name) of fish encountered during sampling for this thesis. Further mentioning will be by the english common name.

Table 3.2.1: Name of fish-species seen in this thesis, with Latin names (WoRMS, 2018) and common names in both English and Norwegian.

Family	**Latin**	**English**	**Norwegian**
Labridae	*Labrus bergylta* (Ascanius, 1767)	Ballan wrasse	Berggylt
(Cuvier, 1816)	*Labrus mixtus* (Linnaeus, 1758)	Cuckoo wrasse	Blåstål/Rødnebb
	Symphodus melops (Linnaeus, 1758)	Goldsinny wrasse	Bergnebb
Gadidae	*Gadus morhua* (Linnaeus, 1758)	Cod	Torsk
(Rafinesque, 1810)	*Pollachius virens* (Linnaeus, 1758)	Saithe	Sei
	Pollachius pollachius (Linnaeus, 1758)	Pollack	Lyr
	Trisopterus minutus (Linnaeus, 1758)	Poor cod	Sypike
	Molva molva (Linnaeus, 1758)	Common ling	Lange
	Raniceps raninus (Linnaeus, 1758)	Tadpole fish	Paddetorsk
	Ciliata spp. (Couch, 1832)	Rockling	Tangbrosme
Miscellaneous	*Ammodytes* spp. (Linnaeus, 1758)	Sand lances	Sil
(Families, genus	Pleuronectidae spp. (Rafinesque, 1810)	Flatfish	Flyndrefisk
& fish species)	Gobiidae spp. (Cuvier, 1816)	Gobies	Kutling
	Gobius niger (Linnaeus, 1758)	Black goby	Svartkutling
	Zoarces viviparus (Linnaeus, 1758)	Viviparous eelpout	Ålekvabbe
	Pholis gunnellus (Linnaeus, 1758)	Rock gunnel	Tangsprell
	Cottidae spp. (Bonaparte, 1831)	Sculpins	Ulkefisk
	Taurulus bubalis (Euphrasen, 1786)	Longspined bullhead	Dvergulke

3.3 Otoliths from shag pellets

The gathered and analyzed otoliths (n = 1397) from the shags regurgitated pellets can be seen in **Figure 3.3.1** as grouped into groups of interest (gadoids and labrids). In further analysis and back-calculation of fish length, Crustacea, Gastropoda and Polychaeta and unidentified fish were excluded. Due to regional findings reported in Hillersøy and Lorentsen (2012), Gadidae indet. were hereafter included in the data-set as saithe. Calculated values can be seen in **Appendix B**. The mean back-calculated fish length of labrids and gadoids were respectively 134.6 mm and 117.3 mm.

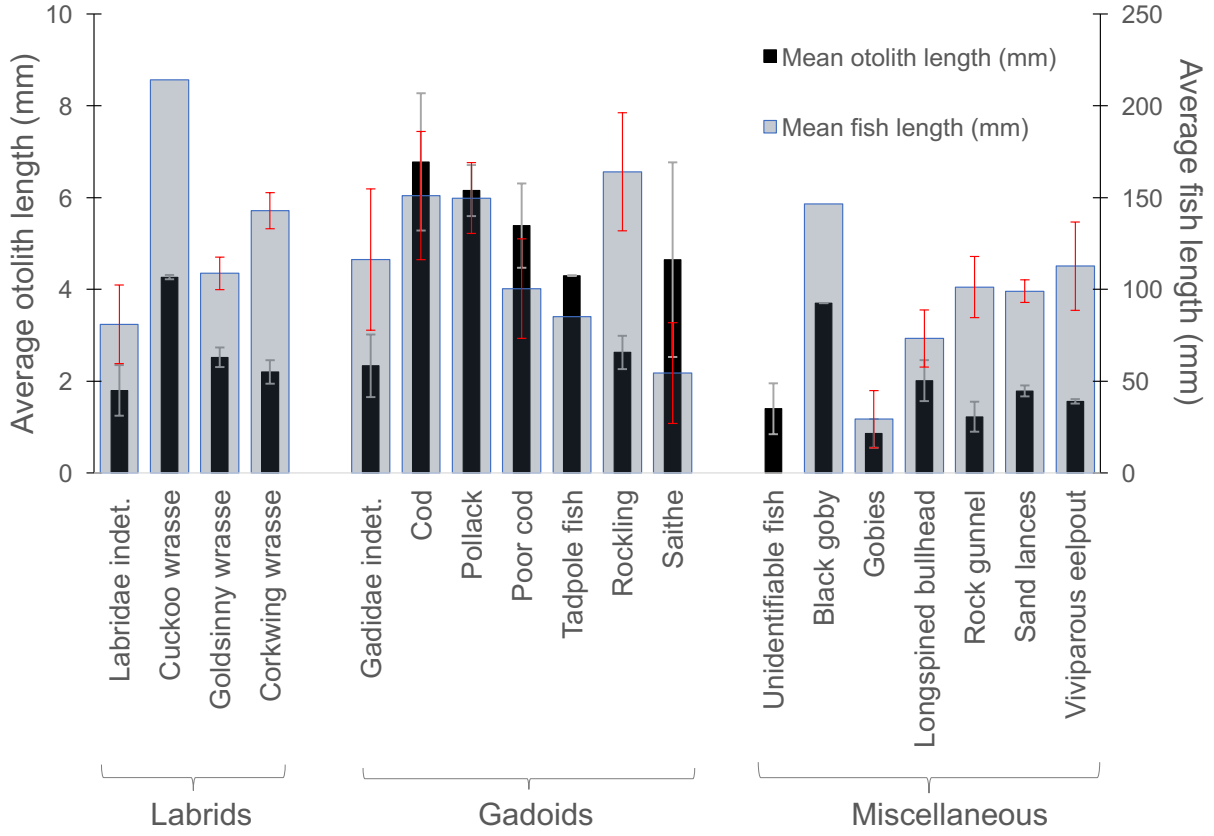

Figure 3.3.1: The unique otoliths (n = 1397) of the gathered pellets where analyzed and determined the specific species of fish. The fish are grouped into Labrids, Gadoids or Miscellaneous. The black bars are the mean otolith lengths (error-bars as standard deviation (SD)) and the light blue bars (with red error-bars as SD) are back-calculated mean fish lengths. No SD was calculated on species with only one otolith (cuckoo wrasse, tadpole fish and black goby). The mean fish length of labrids, gadoids and Miscellaneous were respectively 134.6 mm, 117.3 mm and 93.6 mm. The specified sample group and calculations can be seen in **Table B**, **Appendix B.1**.

3.4 Transect description

3.4.1 Transect #1

The transect followed the shoreline southwards before heading straight west and following the bathymetry down to 32m depth (**Figure 3.4.1**). The kelp forest was dominated by the *Laminaria hyperborea* (Gunnerus, 1766), with many *Saccharina latissima* (Linnaeus, 1753), but also clusters of *Alaria esculenta* (Linnaeus, 1767) and the epiphytic *Palmaria palmata* (Linnaeus, 1753) on the upper parts of *L. hyperborea* stipes in the shallowest parts. From 18 - 23 m only clusters of *L. hyperborea* could be observed, however, deeper than 23 m only bare boulders were observed. This will classify the transect in the EUNIS Habitat classification (seen on **Figure 1.5.1**), hereafter EUNISclass, as A3.15 ("kelp with cushioned fauna and/or foliose red seaweed") going to A4.21 ("echnioderms and crustose communities on circa-littoral rocks") at 23 m depth and greater depths.

3.4.2 Transect #2

The MiniROV was deployed over a traditional fishing-ground for sand lances (**Figure 3.4.2**). The transect, with an average depth of 39m, followed the bathymetry in a southwards direction. There were no observation of fish other than schools of very small and unrecognizable fish species. During the shallower parts of the descent many jellyfish, dominated by *Cyanea capillata*, were observed, while the deepest part of the transect many *Aurelia aurita* were observed. EUNISclass in this transect was classified to A5.25 ("circalittoral fine sand")

3.4.3 Transect #3

The only transect conducted in different parts, and from land, as mentioned in **Section 2.3**. Data from the outer part were excluded due to problems with miniROV-deployment. Data analyzed is from the outermost site and towards the littoral zone, where the first section (**Figure 3.4.3**) was dominated by fine sand and mainly *S. latissima* (some detatched) with some *L. hyperborea* on small rocks. At ~18m the substrate shifted from soft bottom to harder substrate (rocks) and the kelp forest continued to get more dense with the incline. EUNISclasss in the transect was classified to A5.23 ("infralittoral fine sand") at the start of the transect, going to either A3.21 (Kelp and red seaweeds ("moderate energy infralittoral rock") and/or A3.22 ("kelp and seaweed communities in tide-swept sheltered conditions") in the top 18 meters.

3.4.4 Transect #4

Data from instrumented shags (see **Figure 3.1**) showed an area with high amounts of shag dives after excluding dives according to parameters set in **Section 2.4.1**. The transect was conducted in an area where many shags were observed resting and/or drying its feathers along the shoreline. The bathymetry went from fine sand substrate to steep cliffs with sparse

L. hyperborea communities with epigrowth on stipes and lamina (**Figure 3.4.4**). Bathymetry leveled out, and almost no epigrowth could be observed on kelp (mainly *L. hyperborea*). EUNISclass in this transect was classified to A5.25 in the beginning of the transect, and as bathymetry inclined, A3.22 and/or A3.31 ("silted kelp on low energy infralittoral rock with full salinity")

3.4.5 Transect #5

The sand substrate at 25 m depth was covered with spots of debris from detached and degrading tissue of kelp as it seemed like the currents in the area created a gyre-effect on the debris. Many fishes, mainly Gadidae, swam over these spots. Substrate shifted from sand to boulders at ~18 m and was dominated by *L. hyperborea* all the way to the littoral zone. Some *Fucus* indet. (Linnaeus, 1753) were observed close to the surface. EUNISclass was classified to A5.25 in the beginning, going over to either A3.22 and/or A3.31.

The mean length of gadoids was in transects #1, #3, #4 and #5 estimated to be 10-20 cm. The mean length of labrids was in transect #1 estimated to 0-20 cm while transects #3, #4 and #5 were < 10 cm.

3.4.6 Shannon's diversity index

Table 3.4.1 shows the calculated H' and Equitability, according to **Section 2.5.2**, from the observed fish throughout the transects. Calculations can be seen in the Appendix (**Table A** on **page V**).

Table 3.4.1: Calculated Shannon's Diversity Index (H') from the species observed during the transects. Equitability (E) was calculated with a H'_{max} diversity of (n = 1) for every species. Scale of equitability is defined by Jakobsen (2016).

	H'	**E (H'/H'$_{max}$)**	**scale of biodiversity**
Transect #1	0.72	0.65	High
Transect #2	0	0	Not present
Transect #3	0.44	0.39	Medium
Transect #4	0.41	0.37	Medium
Transect #5	0.77	0.69	High

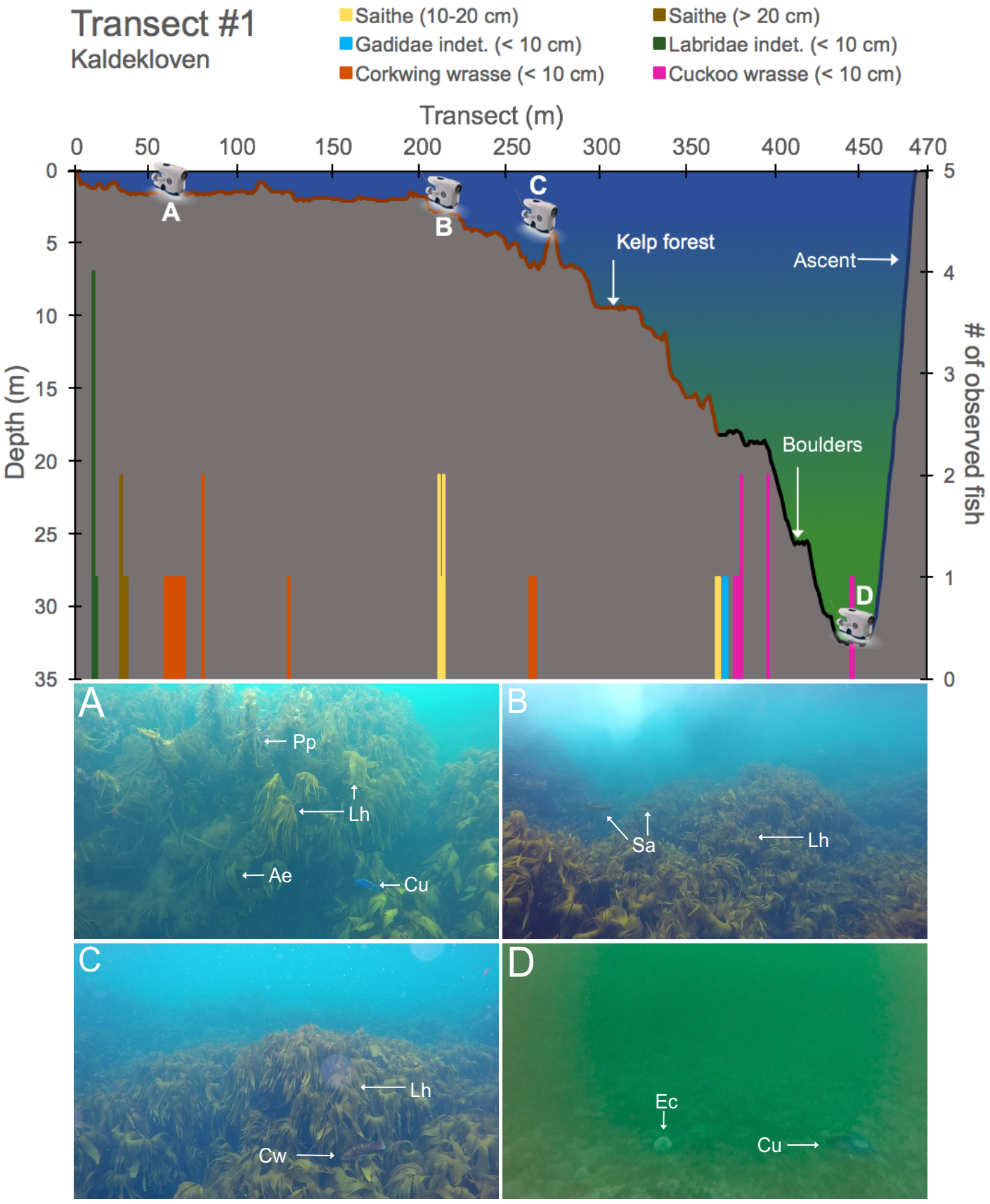

Figure 3.4.1: Fish species diversity and numbers (n = 47) as a function of depth at **ROV Transect #1 - Kaldekloven** (470 m) 22nd of June 2017, 13:30. The primary axis shows the depth profile of the transect and the secondary axis shows numbers of species. The different substrates are indicated within the depth-profile. BluEyes within the figure indicates where in the transect the framegrabs were taken. Observations in ***Mid Panels***: **Site A**: Cuckoo wrasse (Cu) and macroalgal species: *L. hyperborea* (Lh), *A. esculenta* (Ae) and *P. palmata* (Pp). **Site B**: Saithe (Sa) and Lh. ***Lower Panels***: **Site C**: Corckwing wrasse (Cw) and Lh. **Site D** (BluEye footage): Cu and Echinoidae indet.

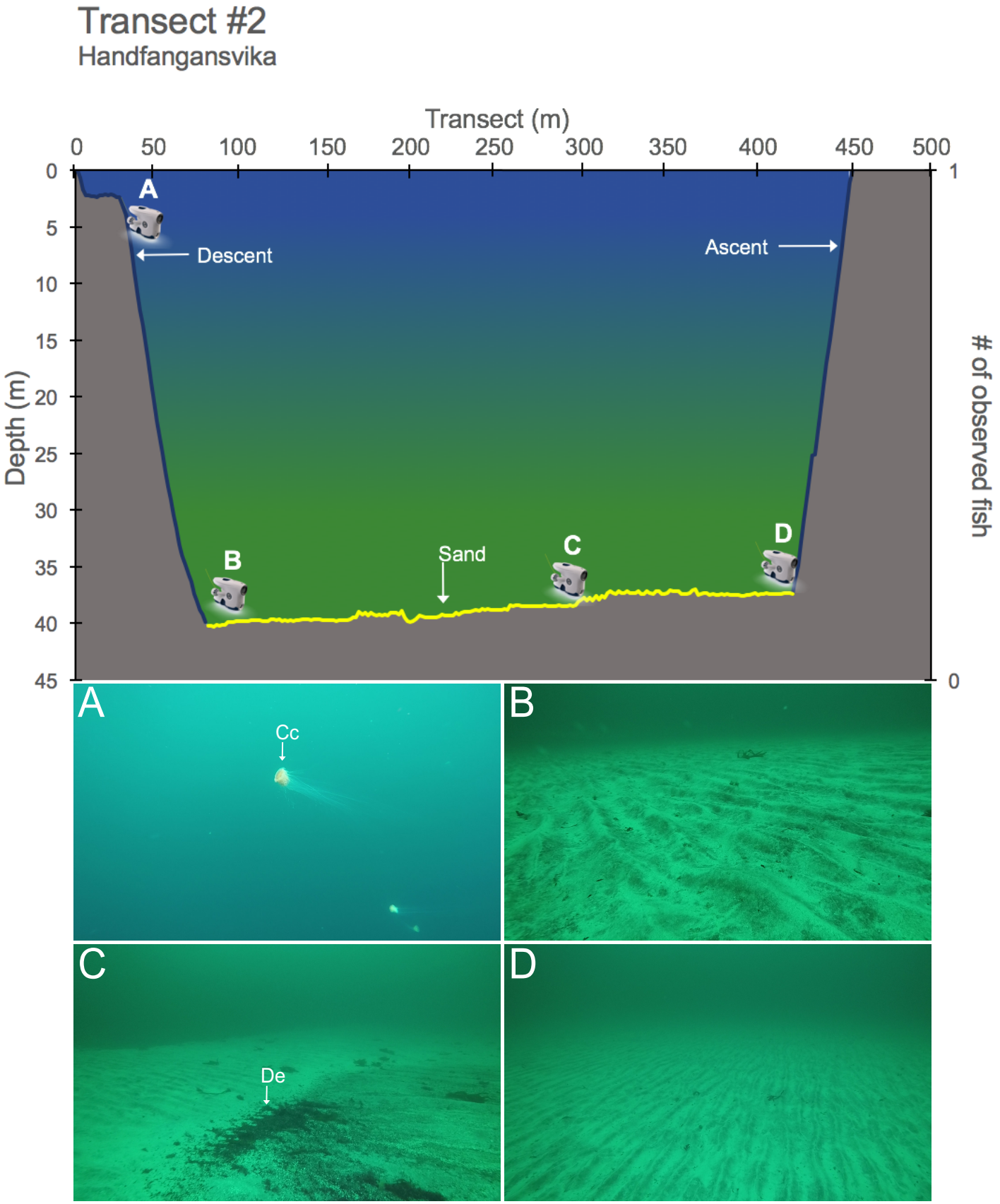

Figure 3.4.2: Fish species diversity and numbers (n = 0) as a function of depth at **ROV Transect #2 - Handfangansvika** (500 m) 22nd of June 2017, 15:30. At this site, no fishes was identified in contrast to habitats with kelp forest. The primary axis shows the depth profile of the transect and the secondary axis shows numbers of species. The different substrates are indicated within the depth-profile. BluEyes within the figure indicates where in the transect the framegrabs were taken. Observations in ***Mid Panels***: **Site A**: *C. capillata* (Cc). ***Lower Panels***: **Site C**: Debris (De) of small particles.

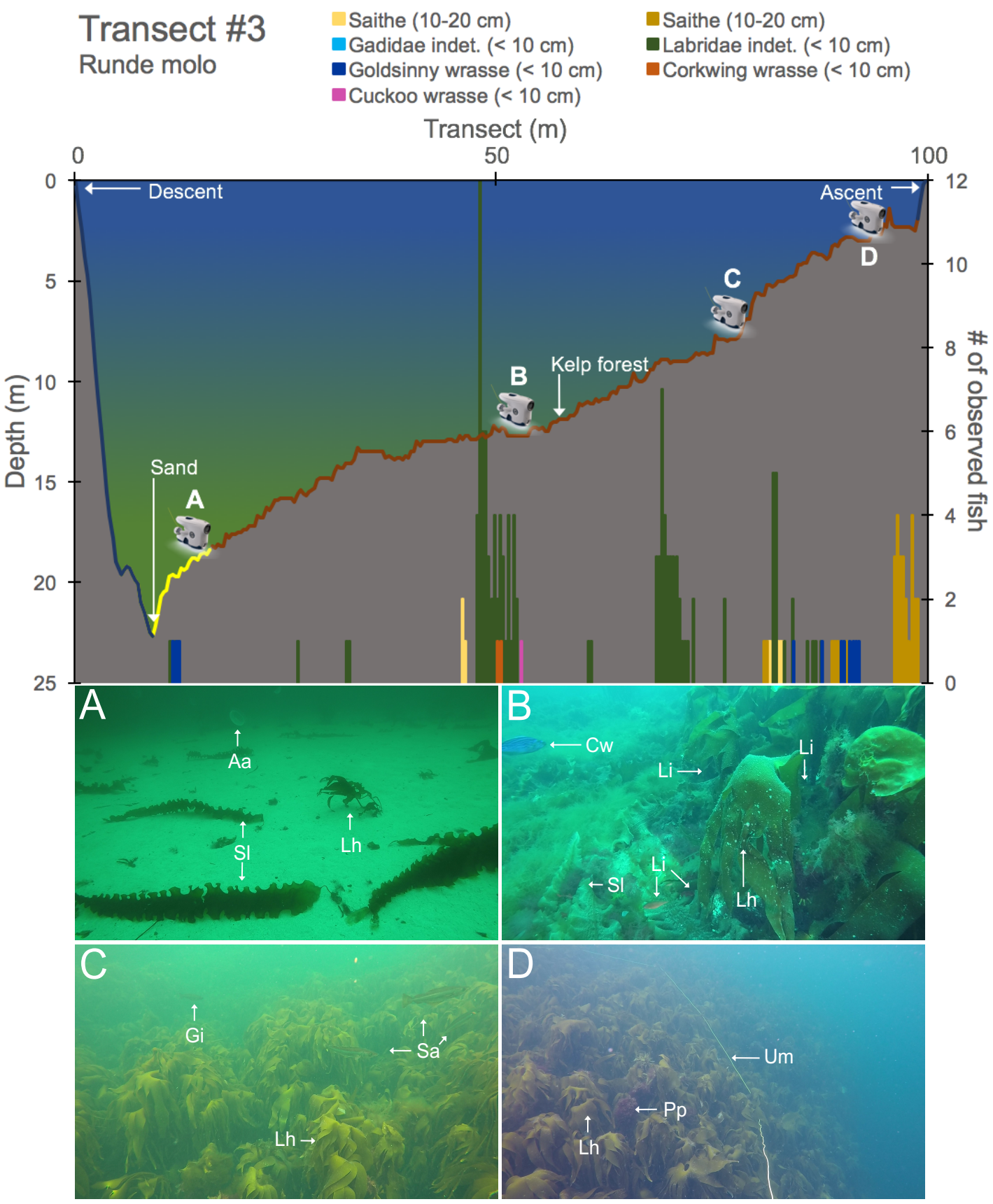

Figure 3.4.3: Fish species diversity and numbers (n = 178) as a function of depth at **ROV Transect #3 - Runde molo** (100 m) 21st of June 2017, 11:00. The primary axis shows the depth profile of the transect and the secondary axis shows numbers of species. The different substrates are indicated within the depth-profile and BluEyes within the figure indicates where in the transect the framegrabs were taken. Observations in ***Mid Panels***: **Site A**: *A. aurita* (Aa) and macroalgal *L. hyperborea* (Lh) and *S. Latissima* (Si). **Site B**: Cuckoo wrasse (Cw), Labridae indet. (Li) and macroalgae Lh and Si. ***Lower Panels***: **Site C**: Saithe (Sa) and Gadidae indet. (Gi) with macroalgae Lh. **Site D**: Lh and *P. palmata* (Pp), while the umbilical (Um) can be seen tangled in Lh.

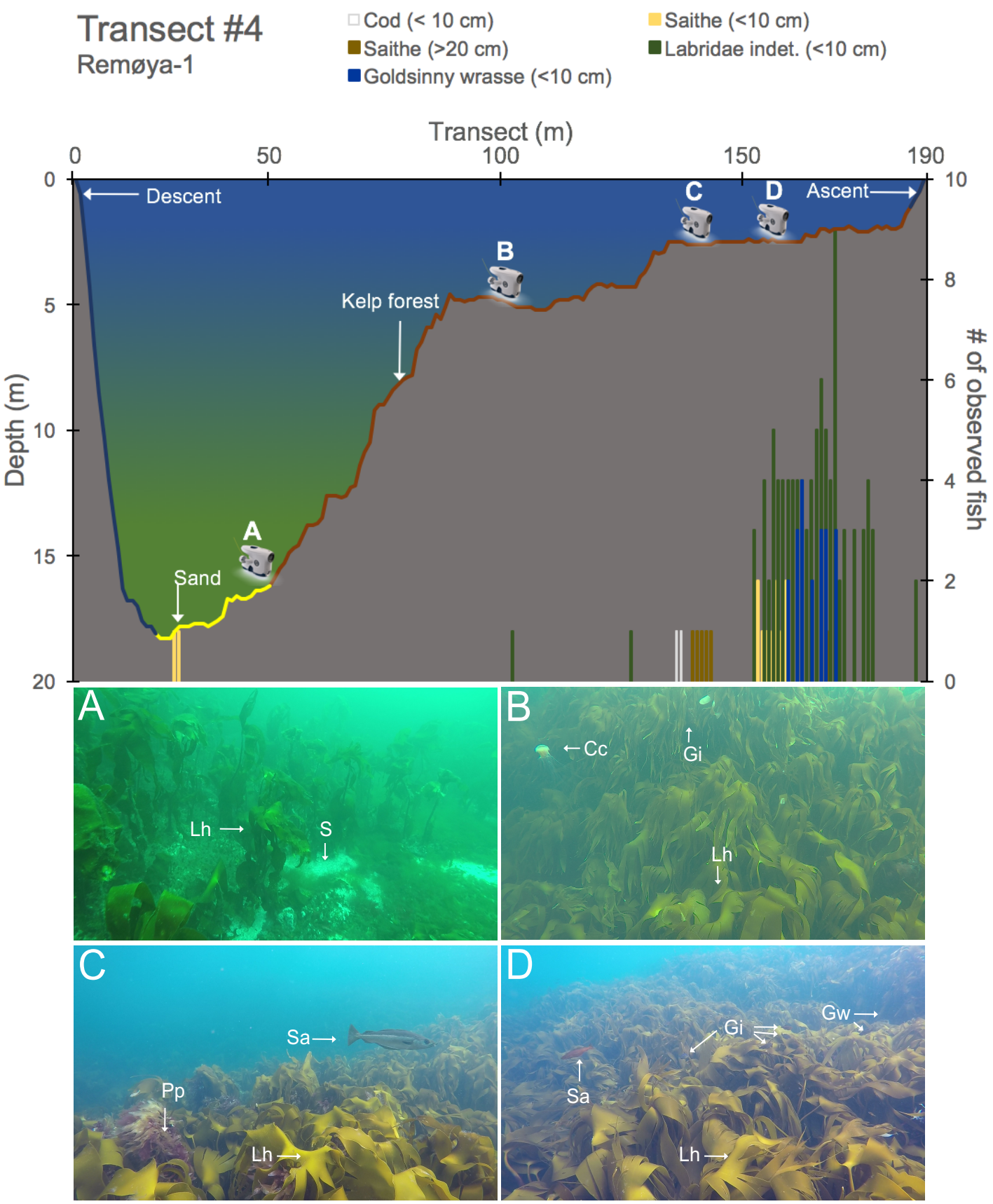

Figure 3.4.4: Fish species diversity and numbers (n = 136) as a function of depth at **ROV Transect #4 - Remøya-1** (190 m) 22nd of June 2017, 10:30. The primary axis shows the depth profile of the transect and the secondary axis shows numbers of species. The different substrates are indicated within the depth-profile. BluEyes within the figure indicates where in the transect the framegrabs were taken. Observations in ***Mid Panels***: **Site A**: *L. hyperborea* (Lh) and patches of sand (S). **Site B**: Gadidae indet. (Gi), *C. capillata* (Cc) and Lh. ***Lower Panels***: **Site C**: Saithe (Sa), Lh and *P. palmata* (Pp). **Site D**: Sa, Gi, Goldsinny wrasse (Gw) and Lh.

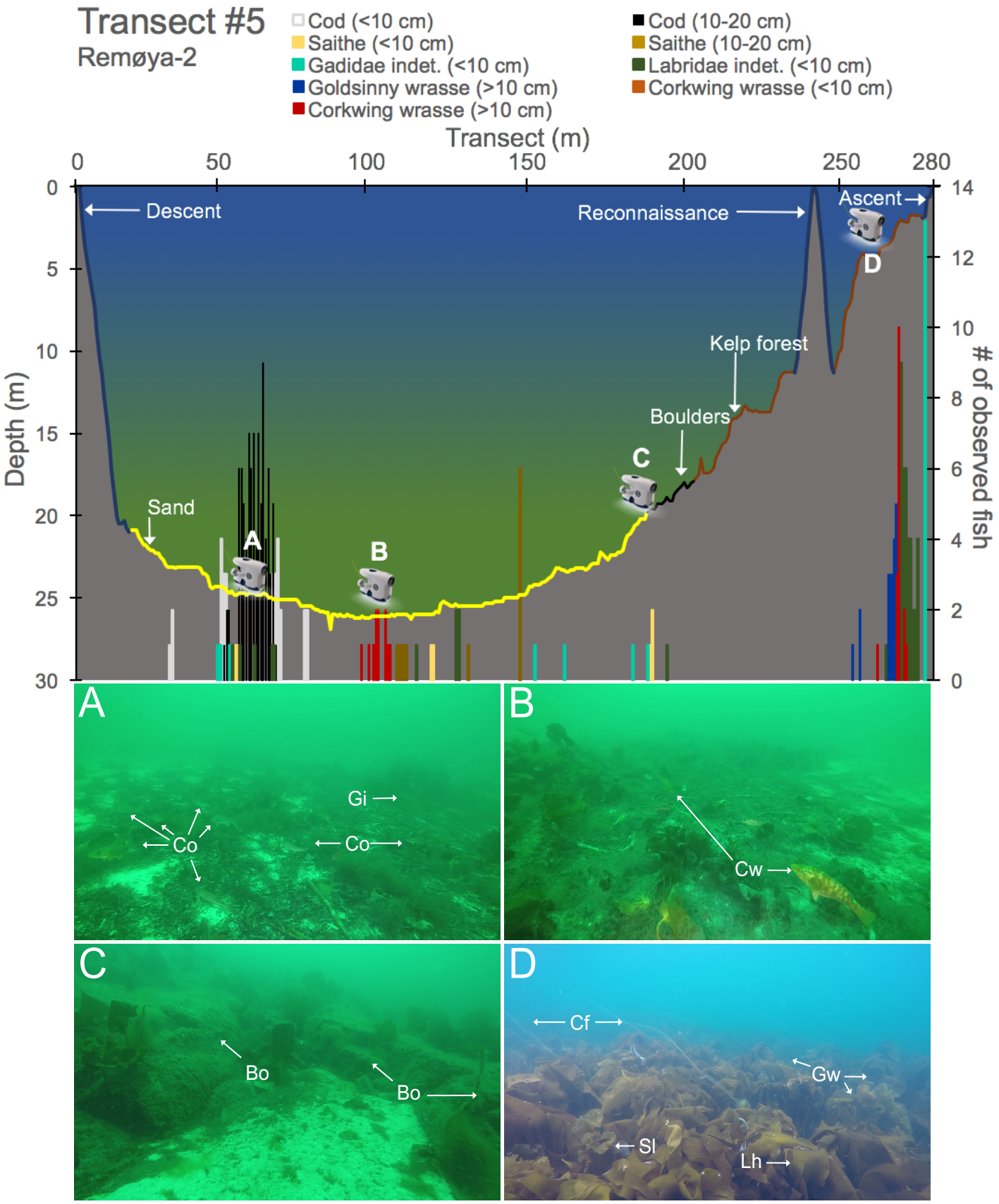

Figure 3.4.5: Fish species diversity and numbers (n = 282) as a function of depth at **ROV Transect #5 - Remøya-2** (280 m) 22nd of June 2017, 12:00. The primary axis shows the depth profile of the transect and the secondary axis shows numbers of species. The different substrates are indicated within the depth-profile. BluEyes within the figure indicates where in the transect the framegrabs were taken. Observations in ***Mid Panels***: **Site A**: Cod (Co) and Gadidae indet (Gi) **Site B**: Corckwing wrasse (Cw). ***Lower Panels***: **Site C**: Boulders (Bo). **Site D**: Goldsinny wrasse (Gw), *L. hyperborea* (Lh), *S. latissima* (Si) and *Chorda filum* (Cf).

4 Discussion

Based on the sampled otoliths (n = 1397), the shags dietary choice comprised of 20 % labrids, 67 % gadoids, 7 % sand lances and 6 % miscellaneous species, and back-calculated mean length of fish was revealed (134.6 mm and 117.3 mm of respectively labrids and gadoids). In an area where shags showed site fidelity (calculated to medium to high scale of biodiversity (H') (see **Table 3.4.1**), biased estimation of fish-length from imagery was 113.0 mm of both labrids and gadoids. GPS-positions of diving shags (n = 861) was logged from instrumented shags (n = 7), revealing areas where shags forage away from the nesting colony (the dive furthest away from the colony was ~14 km). Due to the miniROV nimble and stable design, habitats in exposed-, sheltered,- and near-shore-areas was successfully mapped with EUNIS classification hierarchy. There were big differences in image-quality from the equipped GoPro camera and the miniROV camera, and more fish would have been observed with a higher image-quality and a wider FoV. With higher spatial resolution and larger FoV, this would give more usable data with positioning-technology (geo-referenced) and size measurement tool (scaling of OOI) attached to the miniROV - enabling for a future with preliminary surveys ahead of larger maritime monitoring operations (i.e. habitat mapping and environmental monitoring).

4.1 Instrumented European shags

The mean depth of dives done by European shags in the area of transect #5 as recorded by the TDR-loggers was 20 m ±12 SE, and of all 282 observed fish in the transect, 158 (56.0 %) of total observations were on 23±3 m depth (max depth was 26.3 m). This indicates that the shags were diving at depths where the fish were present. Repeated dives at the same site is however not equivalent to a good foraging area, and could indicate an area where hunting is hard, nevertheless, this survey have no basis to estimate the quality of the foraging area and will not be discussed further. The birds seems to fly to foraging areas in a "commuting" type movement (Kareiva and Odell, 1987; Weimerskirch *et al.*, 1997) showing a foraging site fidelity, which suggests that the bird may know where the food is (Weimerskirch, 2007). The mean foraging range of chick-rearing shags have been found to be 39 km ±0.8 SE and 25 km ±0.8 SE in shag-colonies at respectively Sklinna and Hornøya (Christensen-Dalsgaard *et al.*, 2017). The recorded dive furthest away from the nesting colony at Runde was ~14 km, indicating a foraging range within distances found by Christensen-Dalsgaard *et al.* (2017) at other colonies.

The data from instrumented shags show areas frequently they visited. North of Runde lies "Rundebrandane" (62°25'32.8"N 5°34'46.2"E), see **Figure 2.1.1**; a low-tide elevation (land submerged at high-tide) - and is the most visited area at both low- and high-tide with ~23 % of all recorded dives, their dives tend to be shallower at low-tide and deeper on high-tide. Only 33 % of the GPS- and TDR-recorders attached on shags were recovered, limiting the

sample size to n = 7. From **Figure 3.1.1** there are 243 recorded dive-spots cropped from the figure due to the distance from Runde and the fact that these spots are not included in the sediment map from NGU. The area of "Rundebrandande" is shallow, exposed and not covered by NGU's sediment map. Due to the effect of the weather-conditions during the cruise, this area would be unfavourable to enter with an open work-boat or with "Lophelia", so a sheltered area where the birds also dived was chosen (transects #4 and #5). Other challenges will be discussed in **Section 4.8**

The current recommendation regarding instrument-deployment on birds is that the total weight of instruments should not exceed 3 % of a bird's body mass (Kenward, 1987), and studies on ill-placed and heavy devices have shown that it will change in-flight behavior (Vandenabeele *et al.*, 2014), further increasing both feeding- and flight energy-costs and decreasing the maneuverability of the bird (Adams *et al.*, 2009). Instrumented shags in this survey was well under the recommended maximum payload (1.6 and 1.8 % of body mass), indicating that the birds were not influenced by the instrument deployment and therefore did not change the behaviour of the shags.

4.2 Information gathered from regurgitation pellets

From the analyzed regurgitation pellets from shags on Runde, 20 % of otoliths (n = 1397) was from labrids, 67 % gadoids and 7 % of sand lances. These results from regurgitation pellets are based on the otolith counts and fish species identification, with same trend reported in Barrett *et al.* (1990), where the diet of Norwegian Sea shags by biomass have been found to 70 % gadoids and 15 % sand lances.

The mean back-calculated length of labrids was 134.6 mm, although the mean Labridae indet. (n = 264) was back-calculated to 81.0 mm. The few otoliths from goldsinny-, cuckoo- and corkwing wrasse (respectively n = 10, 1 and 8 and 108.7, 214.1 and 142.8 mm in mean back-calculated body length (see **Table B.1** in **Appendix B**)) increased the mean. The mean length of gadoids was back-calculated to be 117.3 mm, with the highest deviation of Rockling (n = 7 and 164.0 mm (see **Table B.1** in **Appendix B**)).

The number of sand lances otoliths (n = 99) may not represent the entire diet of shags, as small otoliths have been found to be sensitive to erosion from the shags digestive fluids, i.e. stomach acids degrading the calcareous otoliths (Jobling and Breiby, 1986; Ross *et al.*, 2005). Sand lances are an important prey-species for both shags and gadoids due to their high energy content (Harris and Wanless, 1991) (~10 kJ^{-g} of wet weight, while gadoids provides less than half of the energy (~4 kJ^{-g} wet weight) (Barrett *et al.*, 2002)), and decrease in foraged sand lances can be worrisome for the shags future diet as fisheries landings of sand lances continues to increase (Gjøsæter *et al.*, 2008; Johnsen, 2018). The largest recruitment in the first year-class of sand lances was recorded in 2017, and researchers at the Institute of Marine Research (IMR, also known as Havforskningsinstituttet) calculated an increase of 50 % biomass-growth for 2018, however, they reported that 10 % biomass-growth of sand lances,

and one of the major reasons why could be the cold spring of 2018 (3 °C colder than 2017 at 50 m depth), calm spring with low currents or low nutrient upwelling, which may all affect the timing of the phytoplankton springbloom; the primary producers (Hommedal, S., 2018) – which can result in a match/mismatch further up the trophic levels.

The regurgitation pellets collected in the colony was not older than one day [†], hence the pellets represent both time and space (i.e. statistically foraging trips of 7 km away from colony) as this survey. These results will give a good indication of the species and the size of the fish the shags forage on. However, many studies have stated sources of errors in back-calculation of fish size from otolith size, and that the linear otolith-length to fish-length relation may depend on the species growth rate (i.e. Lee Phenomenon, slow growing species tend to have larger otolith), seasonal variations or that otoliths may become curve-linear in some juvenile fishes (Carlander, 1981; Campana, 1990). However, these validations of the result and biases was not taken into consideration in the analysis.

4.3 Video-analysis

Due to the immersion effect/Snell's Law of refraction [††], OOI are 1.3 times larger in water than in air as lights terminal velocity is lower in water (discussed further in **Section 4.7.2** (Ross *et al.*, 1970; Telem and Filin, 2010; Yu *et al.*, 2011). Consequently, size-determinations in the observations in **Section 3.4** will be 1.3 times overestimated. By taking the mean of all observations (i.e. gadoids 15 cm and labrids 5 cm) and consider the refraction of light; the mean gadoid will be 113.0 mm, while the mean labrid will be 38.0 mm. This may fit, as the majority of observations of Labridae indet. were small juveniles in the surface-water (top 5 m). In Transect #5, at depths the shag forage, several labrids 10-20 cm were observed. Considering the refraction of light; the mean size of these will be 113.0 mm as well. The size of the fishes fits with the back-calculated fish sizes in **Section 4.2**.

It is important to note that the bathymetry shown in **Figures 3.4.1**, **3.4.2**, **3.4.3**, **3.4.4** and **3.4.5** is the actual depth of the miniROV, and not the bathymetry in the locality.

4.3.1 EUNIS classification hierarchy

According to the Norwegian Directorate for Nature Management's (DN) Marine Advisory-Handbook (19, 2001 - revised 2007), mapping littoral biodiversity and kelp occurrence is done by using maritime maps, acoustics analysis, field-observations, but mainly mathematically model-based analysis. Further, the habitats of kelp forest have only three categories (1: *L. hyperborea*, 2: *L. hyperborea* mixed with other kelp-species and 3: *Saccharina latissima*) (Rinde *et al.*, 2004). EUNIS, on the other hand, is a highly detailed system, and as this survey just uses the first four of the six levels of the hierarchy (see **Figure 1.5.1**), there are still issues with determination on classification in the upper four levels. The EUNIS-

[†]Information given by the collectors

[††]Also known as Snell–Descartes law and Law of refraction

class used here was defined by EUNIS habitat classification 2007 (Revised descriptions from 2012) (European Environmental Agency, 2018). As an example; Transect #1 have EUNISclass A3.15, which are exposed to high wave action, which typically will support a community of *L. hyperborea* and A4.21 is a habitat that occurs on wave-exposed circalittoral bedrock where Echinoderms (typically for species such as the sea urchin *Echinus esculentus* - see **Figure 3.4.1-D**) and red encrusting calcareous algae. The kelp forest in transects #3, #4 and #5 is hard to define due to the small differences which separates them, and a measurement of the current speed/direction in the area would be a help for further classification. The EUNIS-class system is very complex, however, a EUNISclass-key to classify the habitat to the correct class is available, and when knowing depth, light climate, exposure characteristics (i.e speed of current and wave action), substrate type (and size) and knowing species observed (level 5 and 6) - the key can suggest a given habitat class.

With more time and precise current speed/direction measurements from habitats available, further elaboration of the EUNISclass could be commenced. However, as this was a method to set each transect provided in this thesis into a larger database system and depicting the possibilities using the miniROV, no further elaboration in the EUNISclass was done. Nevertheless, the miniROV is a good tool for gathering information for further habitat classification in the shallowest parts where bigger and more effective mapping tools and vessels can not explore (i.e. see where NGU have not mapped around Runde in **Figure 2.1.1**) and further have this data shared in EMODnet.

4.3.2 The methodology of miniROV transects

The time used per analysis of the frame-grabs varied greatly, with Transect #2 (n = 0 of fish), characterized by only EUNISclass A5.25, being the fastest to process (t = ~0.45 hrs), in contrast to Transect #3 (n = 178 of fish), characterized by EUNISclass A5.23, A3.21 and/or A3.22, being the most complex transect to process (t = ~4 hrs). Required time for analyzing transect imagery depends naturally on the goals of the survey - a rule of thumb is that it takes two to three times longer processing the video-footage than the recording is, this in agreement with Ludvigsen (2010).

As most of the kelp-occurrence in coastal Norway is model-based (as seen in (Bekkby *et al.*, 2002) and (Bekkby *et al.*, 2013)), this survey will argue the need for a standard with a better fit for survey done in shallow water. NS-EN 16260:2012 (standard for visual seabed surveys for collection of environmental data - see further definition in **Section 1.5**) states that the length of a transect mapping a heterogenous habitat should be at least 500 m in length, with frame-grabs more than 20 m apart (which corresponds to one frame per minute at a stable speed of 0.7 knot). As only one of the five transects in this survey was 500 m in length, and for example Transect #3 was 100 m in length (i.e. 5 frame-grabs) - the standard is hard to follow in this type of survey and much information of biodiversity will be lost if the standard was to be followed. Further the NS-standard instruct that for mapping and monitoring surveys on the

biological communities and diversity of flora and megafaunal organisms, species should be identified to lowest possible taxonomic level. Abundances should be recorded as numbers per unit area in the SACFOR (superabundant, abundant, common, frequent, occasional and rare) abundance scale, with nomenclature used from regularly updated literature such as World Register of Marine Species (WoRMS). SACFOR abundance scale was not chosen in this thesis, as just 7 species of fish were categorized.

In contrast, "The Marine Monitoring Handbook" (Davies *et al.*, 2001) (MMH), provides e.g. recommended operating guidelines for "Descriptive and quantitative surveys using remotely operated vehicles". In quantitative ROV surveys, the observed species should be enumerated either along a predefined track, per covered area or per time. MMH further suggests that a given quantitative ROV survey should be enumerated per time if ROVs are maintaining a constant velocity and seabed altitude was problematic. As the miniROV lack a sonar and altimeter (further discussed in **Section 4.7.1**), no seabed altitude is available, and therefore the method of quantitative ROV survey per time was chosen. The time-interval (t = 5 sec) was chosen due to the mean speed of miniROV was estimated to ~0.25 ms^{-1}, giving a frame-grab every ~1.25 m of the transect. The image-quality varies in the footage available (BluEye and GoPro), however was the BluEye-footage chosen due to the advantages of depth/direction-information layered in the footage (see the interface in **Figure 2.2.1**), despite an expectation of higher numbers of observations in GoPro-footage due to the better image-quality (further discussed in **Section 4.3.3**).

To reduce time used to process video footage, several automated processes of fish classifications have emerged, focusing on the fishes texture-features extracted by using statistical moments of gray-level histograms and shape features and silhouette of reef- and demersal fish with various results (Lee *et al.*, 2004; Edgington *et al.*, 2006; Spampinato *et al.*, 2010; Ravanbakhsh *et al.*, 2015; Håpnes, 2015). However, the identification of species based on images is complicated (due to high species diversity and/or small fish are hard to identify), and the success have been with static backgrounds and fish observed from either below or above. However, the shallow coastal waters of Norway are very dynamic, kelp oscillate with the waves, creating a good environment for the fish to blend within habitat (referred to as background matching (Ruxton *et al.*, 2004)) and hide within the kelp canopy. Further, both camera capture exclusively in front of the miniROV, which makes an automated fish classifier depended of a full lateral side for positive identification. As seen in **Figures 3.4.5-A** and **3.4.4-D**, there will be a low probability of fish showing their full detectable lateral side in a frame-grab in a dynamic environment (i.e. within the oscillating kelp-laminas and stipes). Manual post-processing of video-footage will give a higher number of observations as motion breaks background matching, as human eye is more susceptible to detect moving OOI. Furthermore, labrids are known to have many different color morphs and sexual dimorphs (as seen in e.g. corkwing wrasse (Villegas-Ríos *et al.*, 2013; Quintela *et al.*, 2016) and goldsinny wrasse (Uglem *et al.*, 2000; Clark *et al.*, 2016)) and gadoid species is hard to differentiate between the species due to the common morphology (Markle, 1982; Teletchea *et al.*, 2006).

4.3.3 Image quality

The image-quality (especially spatial resolution, contrast and color characteristics) is higher in the GoPro-footage (CMOS-sensor) than the BluEye-footage (CCD-sensor), as can seen in the comparison in **Figure 4.3.1**, consequently more fish may be observed. Nevertheless, 39 % of the fish observed in GoPro-footage is outside the FoV of the BluEye-footage in the figure, arguing that lower observations in BluEye-footage is not just image-quality related, but also point of view- and FoV-related. As seen in **Table 2.2.1**, the GoPro sensor has over 50 % larger horizontal FoV (in air) than the BluEye, thus expectation of a higher numbers of observations using a GoPro-camera is valid.

Figure 4.3.1: Comparison between images taken simultaneously from GoPro- (left) and BluEye footage (right) at 2 m depth (note the white square on the epigrowth of the bryozoan *Membranipora membranacea* (Linnaeus, 1767) on *L. hyperborea* as reference-point in both images (as the two cameras have a different point of view). From the GoPro footage 23 fish are observable, while 10 fish are observable from the BluEye footage - the fish are circled and color-coordinated to observed species/family. Gadidae indet. is black, saithe is orange (dark as the fish is estimated as a large specimen), blue as Labridae indet., purple as goldsinny- and brown as corkwing wrasse. The white dotted line on the GoPro shots indicates the Field of View (FoV) in the BluEye footage.

The miniROVs camera-sensor uses a CCD, where the data is transferred and analogously converted from light-energy hitting the sensor to voltage (charge collected is proportional to its irradiance (μmol quanta of photons m^{-2} s^{-1})) across a pixel array to an output node separated from the pixel, which digitize the analog signal (Debevec and Malik, 1997; Jaffe *et al.*, 2001; Faraji and MacLean, 2006). In contrast, the GoPro camera have a CMOS sensor which comprises of transistors associated to each image-pixel, enabling for each pixel to read out individually - avoiding blur due to over-exposed pixels, which reduce the readout time of the sensor (Weste and Eshraghian, 1994; Lajoinie *et al.*, 2018). CMOS is preferred over CCD due to the faster processing speeds (30 vs. 16 Mbps in respectively GoPro and BluEye - see **Table 2.2.1**) and a lower power-consumption, due to each sensor array of pixels is triggered in a row-sequentially fashion (Jaffe, 1990), also known as “rolling shutter” (Danakis *et al.*, 2012). The faster processing speed in CMOS (due to the fact that shifting of pixel-rows are not necessary (Lajoinie *et al.*, 2018)) enables for higher quality imagery, and theoretically ~twice the quality in a GoPro than in the BluEye-camera. Moreover, in environments with low ambient light intensities (i.e. irradiance), where a high bit resolution (dynamic range of

images) is needed (Nayar and Mitsunaga, 2000), the early CMOS sensors would experience low signal due to low light intensity - resulting in a low signal to noise ratio and ultimately a noisy image (Weste and Eshraghian, 1994; Ludvigsen, 2010). However, CMOS technology is rapidly developing and new CMOS-sensors are more sensitive to light and behave better in low light conditions than CCD-sensors (Villalba *et al.*, 2015; Lajoinie *et al.*, 2018) and CCD-technology has reached its limit, as CMOS technology has succeeding CCD (Luštica, 2011; Villalba *et al.*, 2015; Lajoinie *et al.*, 2018).

In contrast, as the CCD-sensor lacks transistors on each pixel, it is still superior to the traditionally CMOS in terms of noise and dynamic range (Debevec and Malik, 1997; Hain *et al.*, 2007; Villalba *et al.*, 2015). A higher dynamic range (8 bit sensor provide 256 intensities of a given color, while a 12 bit camera obtains 4096 intensity range of a given color) will enhance the probability to identify a fish hiding in the shadows of a lamina. However, a lower value of aperture settings of the front lens ($f2.0$ and $f2.8$ in respectively BluEye and GoPro, see **Table 2.2.1** – $f1.0$ indicates no light loss to image sensor) allows more light through the aperture (i.e. open versus narrow aperture), coupled with a larger image sensor (often then with larger pixel size) will usually result in better light sensitivity (often abbreviated ISO) and spatial resolution (Ludvigsen, 2010; Johnsen *et al.*, 2013). With a higher aperture, the less amount of light passes through the lens (where $f2.0$ is letting 100 % more light through than $f2.8$), giving a higher depth of field (i.e. the narrower the aperture, the higher depth of field (in focus)) at the cost of less light passing through aperture. The GoPro have a more narrow aperture coupled with a larger sensor, resulting in all these effects on light sensitivity almost canceling each other out. Nevertheless, the quality of footage from GoPro is better, with a lower noise ratio than the BluEye.

4.3.4 Underwater images are influenced by AOPs and IOPs

The spectral distribution of light and the quantity (number of photons reaching the camera sensor) will affect the image-quality. Light will be attenuated by inherent optical properties (IOPs) in the water, caused by various concentrations of phytoplankton (Chl a), colored dissolved organic matter (cDOM) and total suspended matter (TSM) will alter the sharpness, colors and contrast of objects due to absorption and/or scattering and/or back-scattering of light (Smith and Baker, 1981; IOCCG, 2000; Johnsen *et al.*, 2009). At greater depths (deeper than 5 m), which was often the case in this survey, the AOPs in ambient light/spectral irradiance also influences the contrast, sharpness and colors of the images. Due to the IOPs in the water, the surface water comprises all wavelengths of visible light (400-700 nm), while at greater depths, such as 20 m, only the green part of the spectrum is left - making identification of fish with aid of colors difficult (Sakshaug *et al.*, 2009; Johnsen *et al.*, 2009) The direction from the ambient light (the sun) will give a diffuse light climate (i.e. linear proprtional with cosine of angle from zenith), furthermore will cloud-cover and waves diffuse and scattering of the ambient light (i.e. flickering effect - focusing and de-focusing of light rays) (McFarland and Loew, 1983; Jaffe, 1990; Sakshaug *et al.*, 2009).

In **Figure 3.4.1-D**, from Transect #1, the influences of apparent optical properties (AOP) are clear. The frame-grab is cropped out (losing the depth/direction interface) from the BluEye-footage at 32 m depth, and all though the frame-grab is through a CCD-sensor, it has a high noise-ratio and not much details are detectable. Moreover, two hours later with less cloud cover (i.e. giving a higher light intensity), the Transect #2 was conducted at mean depth of 40 m with a lower noise-ratio than the shallower Transect #1 (see **Figure 3.4.2-C**), this may be due to the abundance of phytoplankton and zooplankton generally decrease with depth, thus affecting the noise-ratio positively with higher light intensity (Johnsen *et al.*, 2013). Analysis did show that concentration of Chl a (phytoplankton absorbing heavily in the blue and red part of the visible spectrum) decreased as a function of depth at a given location (62.4012 , 5.5888) between the two transects. [†]

To overcome the influences of AOPs and IOPs, ROVs have been equipped with conventionally lighting of incandescent (halogen) or High Intensity Discharge (HID) lamps (Jaffe, 1990), and in more present time LED-lights are used, much due to LEDs have a high luminous efficiency (measured in W m^{-2} (energy per area provided by light source), from 400-700 nm (Thimijan and Heins, 1983), or in Lumens per W (L/w) (Hui and Qin, 2009)). LEDs are capable of both narrow or wide chromatic bandwidths, and have a theoretically efficiency of 220 L/w for a white source (Hardy *et al.*, 2007), while incandescent and HID respectively will have a theoretically efficiency of 10-20 and 120 L/w (Rand *et al.*, 2007). Note howver that lights have evolved significantly the last decade and are much more efficient now.

Due to the spectral dependency of the IOPs in seawater, as discussed, the importance of spectral distribution of light is important, as a result, the output of HID- and LED lights are designed to be in the spectral bands where seawater normally have a lower attenuation (425 - 575 nm) (Volent *et al.*, 2007). The illumination from lamps is further dependent on the seabed altitude, position and distance between OOI and camera (i.e. length of optical path-length that the light travels through), the seawater turbidity affected by light absorption and scattering by Chl a and cDOM and TSM highly affecting the image quality due to changing contrast colors available, and the effect increases with IOPs concentration (Kjerstad, 2014). A high seabed altitude will increase the potential for light attenuation and scattering blurring the images also giving a green hue. When using two light sources, the light beam is directed just out of the cameras FoV, and scattered light will illuminate the FoV (Ludvigsen, 2010). The miniROV is equipped with 10 LED lights specified to 2000 lumen, but at depths explored in this survey, the cameras light sensitivity was higher than the back-scattering of the LEDs. The miniROV light-source (see **Figure 2.2.1a** for miniROV design) is ~20 cm lower than the camera (and ~30 cm below the GoPro); due to the angle from the light source to camera, there were more absorbed and back-scattered light from IOPs (in water column) in the GoPro-footage than in the BluEye-footage. At depths examined in this survey, the preferred illumination mode was with the artificial lights turned off (to avoid scattered light from

[†]Data gathered 21st of June 2017 by Glaucia Fragoso and Geir Johnsen (ENTICE project, NTNU)

IOPs) and only using the ambient light from the sun, which gives less scattered light, but a more narrow wavelength window due to the attenuation of discrete wavelengths (especially in blue and red part of the visible spectrum (400-700 nm)), resulting in imagery dominated within the green spectra (as seen in for example the frame-grabs in **Figures 3.4.2**, **3.4.3** or **3.4.5**.

4.4 Lessons learned from transects

Transect #3 was the only transect conducted from land (see **Figure 2.3.1**), and during the pre-survey of bathymetry, the umbilical entangled in kelp as the miniROV maneuvered down a declining cliff (see **Figure 3.4.3-D**). Nevertheless, the entanglement of the umbilical was resolved quickly due to its positive buoyancy, but it resulted in loss of both the miniROV course and the pilots spatial recognition. At the end of the pre-survey, the miniROV surfaced and an aerial drone obtained the GPS position (start-position for the outer part from an open work-boat) through geo-referenced footage. However, the anchor's cable length was not long enough for anchoring up and a north-easterly current made it hard to maintaining the boats position. Consequently, the outer part of the transect was excluded from further analysis and regarded as a learning experience and testing out the methodology, thus - making the length of umbilical the limiting factor for survey conducted from shore.

In Transect #1 the miniROV quickly descended from 2 m to 32 m depth as it followed the bathymetry from the shallow waters. Information from the habitat was lost, as the majority of the cameras FoV was open waters - and a potential contributor to the low number (n = 47) of observations during the transect. Further, the more exposed a habitat was, the more floating debris (i.e. broken off kelp tissues) could potentially entangle the thrusters of ROV - resulting in maneuverability issues. Furthermore, debris was mistaken for OOI during the exposed transects, which may not have been an issue with a higher image-quality.

The area for Transects #4 and #5 was unknown due to low resolution on nautical charts from the Norwegian Mapping Authority as bigger ships with multi-beam scanning sonar does not sail this close to shore, and for max utilization and gathering of data from a transect in an unknown areas, the need for pre-surveys, as stated in MMH, are important for future studies. As seen in **Figure 3.4.5**, the miniROV had to re-surface for a reconnaissance due to the unknown area and the pilot needed to know if the plotted course was correct.

4.5 Calculated scale of biodiversity

Of the five transects, only #1 and #5 had a high scale of biodiversity (in the scale of equitability defined by (Jakobsen, 2016)), and as previously mentioned, the diversity in Transect #1 could be higher with a different approach. Transects #3 and #4 had a medium scale of biodiversity, despite a high number of observations (n = 178 and 136 respectively), where the majority of observations were of small species of Labridae (68.5 % and 70.7 %, respectively) - giving a low species richness. Moreover, the greater part of Transect #4 was of a cliff-wall, thus -

a medium diversity is within expectations for such a transect. In transect #2 the expected diversity was either not present or low scale of biodiversity, due to the sandbanks in this area are a fishing-ground for sand lances, and adult buries in the sand and juveniles swims in shoals (Johnsen, 2018). Transects #1 and #2 were the longest (470 m and 500 m along the sea floor, respectively), and with the lowest species richness (n = 47 and 0 respectively), however, they were conducted in two different types of habitats (EUNISclass A3.15 and A4.21 in #1 and A5.25 in #2) and directly comparing transects with different length, swath width or habitat could lead to erroneous conclusions and should be avoided (Stirling and Wilsey, 2001; Loiseau *et al.*, 2016).

Further, different species of fish has been shown to respond differently to an approaching ROV, where some species are drawn to the artificial light generated from lamps (Ludvigsen *et al.*, 2018) - giving a positive bias in diversity index calculations, while cod have been found to avoid the lightsource from a ROV (Stoner *et al.*, 2008). The total observations of gadoids in all the five transects (if excluding Transect #5 (with high density of cod)) comprised 97.4 % for saithe and 2.6 % of cod, which may indicate that cod avoid the miniROVs lamps as well, while saithe showed a positive phototaxy behaviour (swim towards a point source of light) at several occasions. Further, juvenile fish was observed avoiding the large specimen of saithe patrolling the kelp forest by hiding in the canopy, making classification of evasive fish hard.

4.6 Advantages with miniROV

The main advantage with the miniROV was the ability to maneuver in areas and waters where conventionally larger sized ROVs and mapping vessels could not, thus enabling for both habitat and bathymetry mapping in the shallower areas from boat or shore, and as seen in **Figure 2.1.1**. As the habitat nor the bathymetry near shore is mapped, the gap of knowledge could be filled with the help of a miniROV. Minor advantages of the miniROV will be further discussed in the next subsections.

4.6.1 Physical restraints and movements

The speed on the miniROV is causing drag forces on the vehicle and the umbilical, which is proportional to the cable length (i.e. operational depth), thus limiting the miniROVs velocity at depth (Ludvigsen, 2010). In **Section 2.2.3**, the theoretically max speed of the miniROV is given to $2 ms^{-1}$, this will decrease with depth. The umbilical bollard pull was noticeable in positive pitch when giving max thrust forwards (i.e. pointing upwards). Nevertheless, the power-to-drag-ratio meant that this was not a big issue, and enabling the miniROV to go to the shallowest parts and to 40 m of depth in a very exposed site. In the longest transects #1 and #2 (470 m and 500 m along sea floor respectively), where the boat had to change its positions to follow the miniROV, it was evident from maneuvering the miniROV that strong currents and pull on the umbilical from the boat would lead to abrupt elevations of the miniROV; showing that the 8 kg miniROV 3-D movements (such as pitch, roll and yaw)

are easily changed due to variables discussed above (i.e. umbilical, length of umbilical, entangled umbilical and current speed/direction etc..).

The latest, and the commercially available version of the miniROV, the BluEye Pioneer, have an extra side-thruster - enabling for moving in the pitch-axis as well. This would eliminate the effect from side-currents, making it easier for the operator to stay on course and to create photo-mosaics.

4.6.2 Creating photo-mosaic

As light attenuation and backscatter issues leads to loss of information as a function of distance the FoV in a camera is limited to a few square meters (Kjerstad, 2014) - a method to overcome this is the photo-mosaic, a compilation of overlapping images to a composite image with extended areal coverage. The method will give detailed imagery of a confined area (Ludvigsen, 2010), and the stable design of the miniROV and the ability to horizontally- and vertically-locking allows it to be stable enough to create photo-mosaics of a vertical area (and seabed with a perpendicular pointed camera). As mentioned, the latest version of the miniROV have an extra side-thruster - this would allow for a greater area to be depicted in a photo-mosaic, by mapping a cliff wall in two axis (up, down and sideways). However, this method was attempted in a steep cliff with *L. hyperborea*-growth and high turbidity, and the miniROV was still stable in the water, nevertheless the kelp oscillated too much for a good photo-mosaic, thus arguing that photo-mosaic in a high-dynamic environment will not work.

4.7 Drawbacks with miniROV

The major drawbacks with using the miniROV BluEye for this type of survey was the lack of positioning and size/length scaling tool, while technical difficulties further discussed was just a minor drawback.

4.7.1 Underwater positioning

Accurate ROV positioning is important for two reasons; knowing where the vehicle is and for geo-referencing of the collected data, thus making it possible to re-visit the habitat for monitoring purposes (time-series). Ludvigsen (2010) states that the importance of knowing the locality for data-gathering is often as important as the data itself (as seen in Transect #4). The two dominating methods for size scaling a ROV position is USBL (Ultra Short Baseline) and LBL (Long Baseline) (Milne, 1983). To attain the position of ROV using a USBL-system, a surface transducer, a mounted heading-, roll- and pitch sensor (IMU) and a dGPS (differential GPS - improved location accuracy) is mounted on the ship, and on the ROV a mounted transponder is required. The surface-transducer sends an acoustic impulse (ping) from the surface which is transponded and sent back from the ROV - from the time used (i.e. speed of sound in water) and angle of returning impulse the position of the ROV can be calculated.

In a LBL-system, an array of transponders placed on the seabed and a transponder mounted on the ROV (Ludvigsen, 2010; Johnsen *et al.*, 2013).

Out of these two systems, a USBL-system would be the easiest way to setup and transport; and follow the "light and nimble" philosophy of the miniROV. As GPS-chips in smartphones and tablets are becoming increasingly accurate, with a theoretically accuracy down to 30 centimeters (with the BCM47755-chip from Broadcom, USA), the internal GPS in the controlling unit of the miniROV can be used as a dGPS for the USBL-system. Further, a IMU/ compass connected to a transducer can hang over the gunwale or into the water from shore-mounted transducer and ping the miniROV - thus, enabling an accurate positioning for the miniROV.

However, the major contributor to error will be the horizontal bearing angle distance from the transceiver to the transponder, and ideally the mother-vessel should be placed directly above the ROV to minimize this error (Ludvigsen, 2010). Therefore, will a shore-mounted transducer have high frequency of error in the geo-positioning - and if the miniROV does descend down a cliff, it will be out of reach for the transducers ping, leaving the data to not be geo-referenced. Thus, will a lightweight IMU off a boats gunwale that follows the miniROV be the best alternative to give good geo-referenced data. Furthermore, the position of miniROV will enable for reference-points in the data gathered, so that much data from the exact same place could be excluded from the data-set.

4.7.2 Scaling of OOI from ROV-based imagery

Video and images lack visual depth in 3 dimensions, and the miniROV have no means of size scaling scale underwater - and as previously discussed, due to the spectral attenuation (narrowing colors available from 400-700 nm) and the corresponding immersion effect (due to different refraction of light underwater at different wavelength) of light underwater a size scaling tool is important for scientific work. Therefore, it is common to use a scaling tool for size and distance size scaling to the depths. Traditionally, a meter-scale placed within the picture was used, but a more convenient and present way of scaling is to mount to or more parallel lasers (with a known distance between, 10 cm is recommended in NS-EN 16260:2012) on the ROV, this would give a length scale on or at the side of OOI. Furthermore, in NS-EN 16260:2012 the standard unit area is given as a 50 x 50 cm frame, which should be marked as a central find on the images after photographing/recording. Due to the miniROV's hull design, it would be possible to mount distance-calibrated lasers on each side of the miniROV. For a perpendicular mounted camera, the scale can be measured off the FoV of the camera and the seabed altitude (gathered using a bathymetry scanning sonar) without the use of lasers (Ludvigsen, 2010). However, as mentioned on the refraction within in-air cameras, scaling with FoV and altitude a more complicated approach.

4.7.3 Technical issues with a ROV-prototype

As the miniROV is a prototype of the commercially available BluEye Pioneer, the software that controls the miniROV is under constant development. The biggest challenges with the miniROV was how the software was coded - some packages of information (i.e. video-stream and control) was lost during the transfer from miniROV to app on the tablet; this was experienced as the feed stopped for a few seconds. The software was encoded as if packages was lost, the information had to be sent again, forcing the video-stream to be played three times the usual speed. This made controlling the miniROV difficult, as when a OOI was in to the FoV and miniROV had to pivot (yaw-axis (i.e. rotate)) to follow the OOI, it was often too late, and the OOI was lost. This was often a issue when diving in a dynamic environment with much movement within the scene. This is important when mapping OOI in a kelp forest due to the movement of the algae (oscillating), differences in current speed and direction, and differences due to the tides.

Other technical issues were when the app crashed (3 times during all 5 transects) and the signal was lost to the miniROV or experienced boot-up issues, not allowing a connection to be established between the app and miniROV. The problem was usually resolved with a hard reboot of tablet or WSU (when the app crashed) or miniROV (when connective issues arose before deploying the the miniROV from mother-vessel). Other challenges with the miniROV was how the software was coded. Some packages of information (i.e. video-stream and control) was lost during transfer from miniROV to app on the tablet; this was experienced as the feed stopped for a few seconds. The software was encoded as if packages was lost, the information had to be sent again, forcing the video-stream to be played three times the usual speed.

4.8 Methodological challenges

During the processing of GPS-data from the instrumented shags, the accuracy of the sensors was questioned. East of transect #2 and north-west of transect #3, two shag dives have been recorded on land despite excluding positions shallower than 1.5 m and speeds $\geq$3 ms^{-1}. This could raise issues with the credibility of the sensors, but all other positions show a clear pattern of areas where the birds are diving. Nevertheless, a high accuracy position for each dive is not needed for this type of study, rather depicting the pattern and area of dives is needed. These two positions makes out 0.002 % of all position, and regarded as outliers in the data-set.

In video analysis, the observations of fish was categorized into different estimated fish sizes. As the miniROV lacked a size scaling tool, the size estimation of fish was in relation to the mean lamina length and area size of *L. hyperborea* and the fishes fraction in the image, making the estimation of the length uncertain. Moreover, when estimating fish sizes without a size scaling tool, the difference of 9 and 11 cm is not apparent - although it is the difference

between two categories. Furthermore, as both cameras are in-air cameras, the refraction-angle of light will differ in water, within the case (air) and lens - making the calculations of refraction complicated (Telem and Filin, 2010), thus highlighting the need for a scaling tool.

Challenges with the method of enumerating per time was when e.g. OOI, anthropogenic objects or debris was observed, the pilot followed or focused on the object - potentially giving a higher number of observed fish, thus a higher scale of biodiversity. However, this could have been avoided if data was geo-referenced and higher image-quality.

The incline from 18 m to 5 m depth depicted in **Figure 3.4.4a** was much steeper than in the figure, due to a slow incline (for testing out the methodology of creating photo-mosaics), many frame-grabs will be recorded at the same depth - giving a flat slope that does not represent the true bathymetry. The flat slope would have been avoided with geo-referenced data.

4.9 Future prospects

The design of the miniROV have proven to work well in both exposed- and sheltered waters, and as seen in **Figure 2.2.1**, the hull design might allow for different technology and sensors attached to the sides of the miniROV.

Marine operations are usually very resource-demanding (cost, time, logistics) and the availability of personnel, vessel, ROV and equipment must be organized before surveys can be initiated. A preliminary survey conducted by a miniROV equipped with a scanning sonar can contribute to a good and cost-effective design of a larger marine operation. And by conducting a collaboration survey with different instrument carrying platforms, valuable cross-disciplinary knowledge can be provided by the miniROV (Ludvigsen *et al.*, 2015). For example can technology like the 180g Micron Scanning Sonar (Tritech International Ltd., UK.) with its maximum range of 75 m and minimum range of 0.3 m be equipped on the miniROV to perform preliminary comprehensive site documentation in e.g. a collaboration survey. The developers of the miniROV have explored depths to 150 m, and the onboard LED light will illuminate only the immediate bathymetry or OOI, and as high-frequency scanning sonars are not dependent on seawater visibility (Ludvigsen *et al.*, 2007), either the camera nor lighting on the miniROV will be a limiting factor for site documentation and they can easily be used for just navigation.

During operations and data-analysis one can get the feeling of a fish is circling the ROV curiously, which can, in diversity studies, give a false impression due to re-counting of the same fish, discussed as “light pollution” by Ludvigsen *et al.* (2018). Also, in post-processing of imagery one might have findings just outside the field of view as the ROV follows its transect-line. These situations can be prevented with mounting a 360 VR camera on either the keel or on top; e.g. Garmin VIRB 360 (Garmin, USA) is a lightweight action-camera which allows for 4K60/5.7K30 360°-footage and will give a whole different spatial resolution.

As the technology of UHI (Underwater Hyperspectral Imaging), where each image pixel gives hyper-spectral reflectance spectra (optical fingerprints per image pixel) and assigned its own contiguous light spectrum, featuring values from all utilized wavelengths, and is used for detecting subtle and unnoticeable spectral properties (Johnsen *et al.*, 2013; Mogstad and Johnsen, 2017)) evolves and the imaging-cameras becomes smaller, the miniROV could be attached with an UHI perpendicularly - making a photo-mosaic of the sea floor. For this to happen, the miniROV must have an altimeter, to ensure fixed seabed-altitude to keep the swath-width at a constant and geo-referenced video. Furthermore, the miniROV have also the potential to be a monitoring device, where it can be attached with different chemical sensors(conductivity, turbidity, pH), fluorometer (fluorescence measurements; i.e. concentration of Chl a) or take water samples (through Niskin bottles for pollutant-analysis).

The autonomy-technology is moving along and there may be a potential into autonomous miniROV in shallow waters as well. One example of technology which may enable for this is Robot Operating System (Quigley *et al.*, 2009), which supports a real-time control, environmental description and collision-free path planning – utilizing sensors such as cameras, sonars and acoustic transponders for a high-precision localization, thus enabling for a safe exploration (Schjølberg and Utne, 2015) if the sensors can be equipped on the miniROV.

5 Conclusion

Instrumented shags (n = 7) logged positions (n = 861) of where, how deep and how long they dived, with fidelity for several areas. The miniROV was deployed in one of the visited areas, and 56 % of all observations were at the same depths the shag dived. The area was calculated to have a medium to high scale of biodiversity through Shannon Diversity Index. From collected pellets in the shag colony, the species compositions (20 % Labridae species, 67 % of Gadidae species and 7 % of sand lances (species within *Ammodytes* genus)) and size was analyzed and back-calculated from otoliths. The mean length of species within families of Labridae and Gadidae was back-calculated to respectively 134.6 mm and 117.3 mm, while the observed mean length, from the miniROV, of both species within Labridae and Gadidae (including the immersion effect of 1.3) was 113.0 mm at the same location as shags foraged. However, can observed length not be verified, as the miniROV lacks a size scaling tool for size and distance.

The different habitats in the five transects was classified using EUNIS habitat classification hierarchy, a more complex system than the Norwegian Directorate for Nature Management's Marine Advisory-Handbook proposes. Transects were conducted accordingly to "The Marine Monitoring Handbook" and not the European Standard NS-EN 16260:2012 (of "Visual seabed surveys using remotely operated and/or towed observation gear for collection of environmental data"). As most of the kelp-occurrence in coastal Norway is model-based, this survey argue the need for a standard with a better fit for surveys done in shallow water. With more time and precise measurements of currents speed/direction available, further elaboration in the hierarchy could have been possible by only using a miniROV.

The imagery from the miniROV included metadata such as time, depth and direction in the interface. However, the image-quality was not good and hard to identify fish species from, and by analyzing the footage, a higher image quality and a wider FoV from the attached GoPro camera, more fish may have been observed, thus giving a higher calculated scale of biodiversity.

The approach was successful as the miniROV could explore and map habitat in exposed-, sheltered- and close to shore-areas, where conventionally larger sized ROVs and mapping vessels can not. It was further a success, as the preferred dietary choices and size (through otolith analysis and back-calculation) of shags was revealed. Furthermore, due to the usage of shags as biological drones, this allowed for the miniROV to follow them from colony to foraging area, observing their preferred dietary choices. The miniROV has a great potential with a better camera-sensor and as an instrument-bearing platform, as several sensor can be attached to the stable hull, giving miniROV geo-referenced data and enabling the miniROV to be used in preliminary survey and monitoring operations (both habitat mapping and monitoring environmental parameters).

6 References

This bibliography uses the reference style of ICES Journal of Marine Science.

Adams, J., Scott, D., McKechnie, S., Blackwell, G., Shaffer, S. A., and Moller, H. 2009. Effects of geolocation archival tags on reproduction and adult body mass of Sooty Shearwaters (*Puffinus griseus*). New Zealand Journal of Zoology, 36: 355–366.

Anker-Nilssen, T., Bakken, V., Strøm, H., Golovkin, A. N., Bianki, V. V., and Tatarinkova, I. P. 2000. The status of marine birds breeding in the Barents Sea region. *In* Rapportserie, vol. 113, p. 213. Norsk Polarinstitutt.

Barrett, R., Røv, N., Loen, J., and Montevecchi, W. 1990. Diets of shags *Phalacrocorax aristotelis* and cormorants *P. carbo* in Norway and possible implications for gadoid stock recruitment. Marine Ecology Progress Series, 66: 205–218.

Barrett, R. T., Anker-Nilssen, T., Gabrielsen, G. W., and Chapdelaine, G. 2002. Food consumption by seabirds in Norwegian waters. ICES journal of Marine Science, 59: 43–57.

Barrett, R. T., Camphuysen, K., Anker-Nilssen, T., Chardine, J. W., Furness, R. W., Garthe, S., Hüppop, O., *et al.* 2007. Diet studies of seabirds: a review and recommendations. ICES Journal of Marine Science, 64: 1675–1691.

Barrett, R. T. and Furness, R. W. 1990. The prey and diving depths of seabirds on Hornøy, North Norway after a decrease in the Barents Sea capelin stocks. Ornis Scandinavica, 21: 179–186.

Barrett, R. T., Lorentsen, S.-H., and Anker-Nilssen, T. 2006. The status of breeding seabirds in mainland Norway. Atlantic Seabirds, 8: 97–126.

Bekkby, T., Erikstad, L., Bakkestuen, V., and Bjørge, A. 2002. A landscape ecological approach to coastal zone applications. Sarsia: North Atlantic Marine Science, 87: 396–408.

Bekkby, T., Moy, F. E., Olsen, H., Rinde, E., Bodvin, T., Bøe, R., Steen, H., *et al.* 2013. The Norwegian Programme for Mapping of Marine Habitats–Providing Knowledge and Maps for ICZMP. *In* Global Challenges in Integrated Coastal Zone Management, edited by S. J. Moksness E, Dahl E, chap. 2, pp. 21–30. John Wiley & Sons, Oxford.

Bekkby, T., Rinde, E., Erikstad, L., and Bakkestuen, V. 2009. Spatial predictive distribution modelling of the kelp species *Laminaria hyperborea*. ICES Journal of Marine Science, 66: 2106–2115.

BluEye.no 2018. *BluEye Pioneer*. [online] Available at: https://www.blueye.no, (Accessed: January 16th 2018).

Borcard, D., Legendre, P., Avois-Jacquet, C., and Tuomisto, H. 2004. Dissecting the spatial structure of ecological data at multiple scales. Ecology, 85: 1826–1832.

Brass, G., Southam, J., and Peterson, W. 1982. Warm saline bottom water in the ancient ocean. Nature, 296: 620.

Broecker, W. S. 1991. The Great Ocean Conveyor. Oceanography, 4: 79–89.

Brown, C. J., Smith, S. J., Lawton, P., and Anderson, J. T. 2011. Benthic habitat mapping: A review of progress towards improved understanding of the spatial ecology of the seafloor using acoustic techniques. Estuarine, Coastal and Shelf Science, 92: 502–520.

Buhl-Mortensen, L., Buhl-Mortensen, P., Dolan, M. F., and Holte, B. 2015. The MAREANO programme – A full coverage mapping of the Norwegian off-shore benthic environment and fauna. Marine Biology Research, 11: 4–17.

Burgess, M. D., Smith, K. W., Evans, K. L., Leech, D., Pearce-Higgins, J. W., Branston, C. J., Briggs, K., *et al.* 2018. Tritrophic phenological match–mismatch in space and time. Nature ecology & evolution, p. 1.

Calewaert, J.-B., Weaver, P., Gunn, V., Gorringe, P., and Novellino, A. 2016. The European marine data and observation network (EMODnet): your gateway to European marine and coastal data. *In* Quantitative Monitoring of the Underwater Environment, pp. 31–46. Springer.

Campana, S. E. 1990. How reliable are growth back-calculations based on otoliths? Canadian Journal of Fisheries and Aquatic Sciences, 47: 2219–2227.

Campana, S. E. 2001. Accuracy, precision and quality control in age determination, including a review of the use and abuse of age validation methods. Journal of fish biology, 59: 197–242.

Campana, S. E. and Thorrold, S. R. 2001. Otoliths, increments, and elements: keys to a comprehensive understanding of fish populations? Canadian Journal of Fisheries and Aquatic Sciences, 58: 30–38.

Carlander, K. D. 1981. Caution on the use of the regression method of back-calculating lengths from scale measurements. Fisheries, 6: 2–4.

Christensen-Dalsgaard, S., Mattisson, J., Bekkby, T., Gundersen, H., May, R., Rinde, E., and Lorentsen, S.-H. 2017. Habitat selection of foraging chick-rearing European shags in contrasting marine environments. Marine Biology, 164: 196.

Christie, H., Jørgensen, N. M., Norderhaug, K. M., and Waage-Nielsen, E. 2003. Species distribution and habitat exploitation of fauna associated with kelp (*Laminaria hyperborea*) along the Norwegian coast. Journal of the Marine Biological Association of the United Kingdom, 83: 687–699.

Clark, W., Leclercq, E., Migaud, H., Nairn, J., and Davie, A. 2016. Isolation, identification and characterisation of Ballan wrasse *Labrus bergylta* plasma pigment. Journal of fish biology, 89: 2070–2084.

Cramp, S. and Perrins, C. 1983. The birds of the western Palearctic, Vol. III. Oxford University Press, Oxford., 19: 183–206.

Cury, P. M., Boyd, I. L., Bonhommeau, S., Anker-Nilssen, T., Crawford, R. J., Furness, R. W., Mills, J. A., *et al.* 2011. Global seabird response to forage fish depletion—one-third for the birds. Science, 334: 1703–1706.

Cushing, D. H. 1982. Climate and fisheries. Academic Press, London.

Cushing, D. H. 1990. Plankton production and year-class strength in fish populations: an update of the match/mismatch hypothesi. *In* Advances in Marine Biology, vol. 26, pp. 249–293. Elsevier.

Danakis, C., Afgani, M., Povey, G., Underwood, I., and Haas, H. 2012. Using a CMOS camera sensor for visible light communication. *In* Globecom Workshops, pp. 1244–1248. IEEE.

Davies, C. E., Moss, D., and Hill, M. O. 2004. EUNIS habitat classification revised 2004. Report to: European Environment Agency-European Topic Centre on Nature Protection and Biodiversity, pp. 127–143.

Davies, J., Baxter, J., Bradley, M., Connor, D., Khan, J., Murray, E., Sanderson, W., *et al.* 2001. Marine Monitoring Handbook. Joint Nature Conservation Committee, p. 221.

Debevec, P. E. and Malik, J. 1997. Recovering high dynamic range radiance maps from photographs. *In* Proceedings of the 24th annual conference on Computer graphics and interactive techniques, pp. 369–378. ACM Press/Addison-Wesley Publishing Co.

Descamps, S., Aars, J., Fuglei, E., Kovacs, K. M., Lydersen, C., Pavlova, O., Pedersen, Å. Ø., *et al.* 2017. Climate change impacts on wildlife in a High Arctic archipelago – Svalbard, Norway. Global change biology, 23: 490–502.

Doney, S. C. 2006. Oceanography: Plankton in a warmer world. Nature, 444: 695.

Durant, J. M., Hjermann, D. Ø., Anker-Nilssen, T., Beaugrand, G., Mysterud, A., Pettorelli, N., and Stenseth, N. C. 2005. Timing and abundance as key mechanisms affecting trophic interactions in variable environments. Ecology Letters, 8: 952–958.

Durant, J. M., Hjermann, D. Ø., Ottersen, G., and Stenseth, N. C. 2007. Climate and the match or mismatch between predator requirements and resource availability. Climate research, 33: 271–283.

Durant, J. M., Stenseth, N. C., Anker-Nilssen, T., Harris, M. P., Thompson, P. M., and Wanless, S. 2004. Marine birds and climate fluctuation in the North Atlantic. Marine ecosystems and climate variation: the North Atlantic, pp. 95–105.

Edgington, D. R., Cline, D. E., Davis, D., Kerkez, I., and Mariette, J. 2006. Detecting, tracking and classifying animals in underwater video. *In* OCEANS, pp. 1–5. IEEE.

Edwards, M. and Richardson, A. J. 2004. Impact of climate change on marine pelagic phenology and trophic mismatch. Nature, 430: 881–884.

European Commission 2008. Directive 2008/56/EC of the European Parliament and of the Council establishing a framework for community action in the field of marine environmental policy. Official Journal of the European Union), 164: 19–40.

European Environmental Agency 2018. EUNIS habitat classification. [online] Available at: https://www.eea.europa.eu/data-and-maps/data/eunis-habitat-classification#tab-based-on-data, (Accessed: May 16th 2018).

Faraji, H. and MacLean, W. J. 2006. CCD noise removal in digital images. Transactions on image processing, 15: 2676–2685.

Fauchald, P., Anker-Nilssen, T., Barrett, R., Bustnes, J. O., Bårdsen, B.-J., Christensen-Dalsgaard, S., Descamps, S., *et al.* 2015. The status and trends of seabirds breeding in Norway and Svalbard. NINA rapport 1151. Norwegian Institute for Nature Research, Trondheim.

Fjøsne, K. and Gjøsæter, J. 1996. Dietary composition and the potential of food competition between 0-group cod (*Gadus morhua* L.) and some other fish species in the littoral zone. ICES Journal of Marine Science, 53: 757–770.

Francis, R. 1990. Back-calculation of fish length: a critical review. Journal of Fish Biology, 36: 883–902.

Geological Survey of Norway 2018. *Datasheet: N25 Detailed Sediment Map*. [online] Available at: http://www.ngu.no/upload/Kartkatalog/Produktark_Marin_SedimentKornstorrelse_Det.pdf (Accessed: March 23rd 2018).

Gjøsæter, H., Huse, G., Robberstad, Y., and Skogen, M. D. 2008. Havets ressurser og miljø 2008. Fisken og havet, Særnummer 1-2008: 34–36.

Glagla, P. 2017. ImageGrab version 5.0.7. [online] Available at: http://paul.glagla.free.fr/imagegrab_en.htm (Accessed: January 17th 2018).

Godø, O., Gjøsæter, J., Sunnanå, K., and Dragesund, O. 1989. Spatial distribution of 0-group gadoids off mid-Norway. *In* ICES Marine Science Symposia. 1989, vol. 191, pp. 273–280.

Gundersen, H., Norderhaug, K. M., Christie, H. C., Moy, F. E., Hjermann, D. Ø., Vedal, J., Ledang, A. B., *et al.* 2014. Tallknusing av sukkertaredata. Norsk Institutt for Vannforskning, 6737-2014.

Hain, R., Kähler, C. J., and Tropea, C. 2007. Comparison of CCD, CMOS and intensified cameras. Experiments in fluids, 42: 403–411.

Hairston, N. G., Smith, F. E., and Slobodkin, L. B. 1960. Community structure, population control, and competition. The american naturalist, 94: 421–425.

Håpnes, S. J. H. 2015. Mapping of demersal fish and benthos by Autonomous Underwater Vehicle equipped with optical and acoustic imagers at 600 meters depth in Trondheimsfjorden. Master's thesis, NTNU, Institute for Biology.

Hardy, K. R., Olsson, M., Sanderson, J., Steeves, K., Lakin, B., Simmons, J., and Weber, P. 2007. High brightness light emitting diodes for ocean applications. *In* OCEANS, pp. 1–4. IEEE.

Härkönen, T. 1986. Guide to the otoliths of the bony fishes of the Northeast Atlantic. Hellerup, Denmark: Danbiu ApS. Biological consultants.

Harris, M. and Wanless, S. 1991. The importance of the lesser sandeel ammodytes marinus in the diet of the shag phalacrocorax aristotelis. Ornis Scandinavica, pp. 375–382.

Hill, M. O. 1973. Diversity and evenness: a unifying notation and its consequences. Ecology, 54: 427–432.

Hillersøy, G. and Lorentsen, S.-H. 2012. Annual variation in the diet of breeding european shag (phalacrocorax aristotelis) in central norway. Waterbirds, 35: 420–429.

Holland, G. J., Greenstreet, S. P., Gibb, I. M., Fraser, H. M., and Robertson, M. R. 2005. Identifying sandeel *Ammodytes marinus* sediment habitat preferences in the marine environment. Marine Ecology Progress Series, 303: 269–282.

Hommedal, S. 2018. Uvanleg tynn tobis overraskar forskarane. [online] Available at: https://www.hi.no/hi/nyheter/2018/mai/uvanleg-tynn-tobis-overraskar-forskarane, (Accessed: May 16th 2018).

Hui, S. and Qin, Y. 2009. A general photo-electro-thermal theory for light emitting diode (LED) systems. Transactions on Power electronics, 24: 1967–1976.

ICES 2017. WGMHM - Report of the Working Group on Marine Habitat Mapping. Working Group on Marine Habitat Mapping, ICES CM 2001/E: 07: 43 pages.

IOCCG 2000. Remote sensing of ocean colour in coastal, and other optically-complex, waters. Reports of the International Ocean-Colour Coordinating Group, No. 3, pp. 22–25.

IPCC 2013. Climate Change 2013: The physical science basis: Working Group II Contribution to the IPCC 5th Assessment report. Cambridge University Press.

Jaffe, J. S. 1990. Computer modeling and the design of optimal underwater imaging systems. Journal of Oceanic Engineering, 15: 101–111.

Jaffe, J. S., Moore, K. D., McLean, J., and Strand, M. P. 2001. Underwater optical imaging: status and prospects. Oceanography, 14: 66–76.

Jakobsen, J. 2016. The Tautra Cold-Water Coral Reef-Mapping and describing the biodiversity of a cold-water coral reef ecosystem in the Trondheimsfjord by use of multi-beam echo sounding and video mounted on a remotely operated vehicle. Master's thesis, NTNU, Institute for Biology.

Jensen, A. 1998. The seaweed resources of Norway. *In* Seaweed Resources of the World, edited by A. T. Critchely and M. Ohno, pp. 200–209. Japan International Cooperation Agency.

Jobling, M. and Breiby, A. 1986. The use and abuse of fish otoliths in studies of feeding habits of marine piscivores. Sarsia, 71: 265–274.

Johnsen, E. 2018. Foreløpige råd for tobisfiskeriet i norsk økonomisk sone 2018. [online] Available at: http://www.imr.no, (Accessed: May 14th 2018).

Johnsen, G., Ludvigsen, M., Sørensen, A., and Aas Sandvik, L. M. 2016. The use of underwater hyperspectral imaging deployed on remotely operated vehicles-methods and applications. IFAC-PapersOnLine, 49: 476–481.

Johnsen, G., Volent, Z., Dierssen, H., Pettersen, R., Van Ardelan, M., Søreide, F., Fearns, P., *et al.* 2013. Underwater hyperspectral imagery to create biogeochemical maps of seafloor properties. *In* Subsea optics and imaging, pp. 508–540e. Elsevier.

Johnsen, G., Volent, Z., Sakshaug, E., Sigernes, F., and Pettersson, L. 2009. Remote sensing in the Barents Sea. *In* Ecosystem Barents Sea, edited by E. Sakshaug, G. Johnsen, and K. Kovavs, chap. 6, pp. 139–166. Tapir Academic Press, Trondheim.

Jost, L. 2006. Entropy and diversity. Oikos, 113: 363–375.

Kain, J. M. 1971. Synopsis of biological data on *Laminaria hyperborea.* Food and Agriculture Organization of the United Nations. Fish. Synopsis No. 87.

Kareiva, P. and Odell, G. 1987. Swarms of predators exhibit "preytaxis" if individual predators use area-restricted search. The American Naturalist, 130: 233–270.

Keats, D., Steele, D., and South, G. 1987. The role of fleshy macroalgae in the ecology of juvenile cod (*Gadus morhua* L.) in inshore waters off eastern Newfoundland. Canadian Journal of Zoology, 65: 49–53.

Kenward, R. E. 1987. Wildlife radio tagging: Equipment, field techniques and data analysis. Symposium of the Zoological Society of London, 49: 175–196.

Keogan, K., Daunt, F., Wanless, S., Phillips, R. A., Walling, C. A., Agnew, P., Ainley, D. G., *et al.* 2018. Global phenological insensitivity to shifting ocean temperatures among seabirds. Nature Climate Change, 8: 313.

Kjerstad, I. 2014. Underwater Imaging and the effect of inherent optical properties on image quality. Master's thesis, NTNU, Institute for Biology.

Klemsdal, T. 1982. Coastal classification and the coast of Norway. Norwegian Journal of Geography, 36: 129–152.

Kroeker, K. J., Kordas, R. L., Crim, R., Hendriks, I. E., Ramajo, L., Singh, G. S., Duarte, C. M., *et al.* 2013. Impacts of ocean acidification on marine organisms: quantifying sensitivities and interaction with warming. Global change biology, 19: 1884–1896.

Lajoinie, G., de Jong, N., and Versluis, M. 2018. Brandaris ultra high-speed imaging facility. *In* The Micro-World Observed by Ultra High-Speed Cameras, edited by T. Kinko, pp. 49–77. Springer.

Lee, D.-J., Schoenberger, R. B., Shiozawa, D., Xu, X., and Zhan, P. 2004. Contour matching for a fish recognition and migration-monitoring system. *In* Two-and Three-Dimensional Vision Systems for Inspection, Control, and Metrology II, vol. 5606, pp. 37–49. International Society for Optics and Photonics.

Lee, R. M. 1920. A review of the methods of age and growth determination in fishes by means of scales. Fishery Invest., 4: 32.

Loiseau, N., Gaertner, J.-C., Kulbicki, M., Merigot, B., Legras, G., Taquet, M., and Gaertner-Mazouni, N. 2016. Assessing the multicomponent aspect of coral fish diversity: The impact of sampling unit dimensions. Ecological indicators, 60: 815–823.

Lorentsen, S.-H. 2005. Det nasjonale overvåkningsprogrammet for sjøfugl. resultater til og med hekkesesongen. NINA Rapport 97. Norwegian Institute for Nature Research, Trondheim.

Lorentsen, S.-H., Anker-Nilssen, T., Erikstad, K. E., and Røv, N. 2015. Forage fish abundance is a predictor of timing of breeding and hatching brood size in a coastal seabird. Mar Ecol Prog Ser, 519: 209–220.

Loya, Y. 1978. Plotless and transect methods. *In* In Coral Reefs: Research Methods, edited by D. R. Stoddart and R. E. Johannes, pp. 197–217. UNESCO, Paris.

Ludvigsen, M. 2010. An ROV toolbox for optical and acoustical seabed investigations. Ph.D thesis, Norwegian University of Science and Technology, Faculty of Engineering Science and Technology, Department of Marine Technology.

Ludvigsen, M., Berge, J., Geoffroy, M., Cohen, J. H., Pedro, R., Nornes, S. M., Singh, H., *et al.* 2018. Use of an Autonomous Surface Vehicle reveals small-scale diel vertical migrations of zooplankton and susceptibility to light pollution under low solar irradiance. Science advances, 4: eaap9887.

Ludvigsen, M., Johnsen, G., Sørensen, A. J., Lågstad, P. A., and Ødegård, Ø. 2014. Scientific operations combining ROV and AUV in the Trondheim Fjord. Marine Technology Society Journal, 48: 59–71.

Ludvigsen, M., Sortland, B., Johnsen, G., and Singh, H. 2007. Applications of geo-referenced underwater photo mosaics in marine biology and archaeology. Oceanography, 20: 140–149.

Ludvigsen, M., Thorsnes, T., Hansen, R. E., Sørensen, A. J., Johnsen, G., Lågstad, P. A., Ødegård, Ø., *et al.* 2015. Underwater vehicles for environmental management in coastal areas. *In* OCEANS, pp. 1–6. IEEE.

Luštica, A. 2011. CCD and CMOS image sensors in new HD cameras. *In* ELMAR Proceedings, pp. 133–136. IEEE.

Manahan, S. 2017. Water Chemistry – Green Science and Technology of Nature's Most Renewable Resource. CRC press, London.

Markle, D. F. 1982. Identification of larval and juvenile canadian atlantic gadoids with comments on the systematics of gadid subfamilies. Canadian Journal of Zoology, 60: 3420–3438.

McFarland, W. N. and Loew, E. R. 1983. Wave produced changes in underwater light and their relations to vision. Environmental Biology of Fishes, 8: 173–184.

McLusky, D. and Sargent, J. 1990. Trophic relationships in the marine environment—summary and way forward. *In* Trophic Relationships in the Marine Environment, edited by M. Barnes and R. N. Gibson, pp. 597–599. Aberdeen University Press, Aberdeen.

Milne, P. H. 1983. Underwater acoustic positioning systems. Gulf Publishing Co., Houston, TX, USA.

Mogstad, A. A. and Johnsen, G. 2017. Spectral characteristics of coralline algae: a multi-instrumental approach, with emphasis on underwater hyperspectral imaging. Applied Optics, 56: 9957–9975.

Mosegaard, H., Svedäng, H., and Taberman, K. 1988. Uncoupling of somatic and otolith growth rates in arctic char (salvelinus alpinus) as an effect of differences in temperature response. Canadian Journal of Fisheries and Aquatic Sciences, 45: 1514–1524.

Muus, B., Nielsen, J., Dahlstrom, P., and Nystrom, B. 1999. Sea fish. Scandinavian Fishing Year Book–Hedehusene. Narayana Press, Odder, 340 pp.

Nayar, S. K. and Mitsunaga, T. 2000. High dynamic range imaging: Spatially varying pixel exposures. *In* Proceedings. Conference on Computer Vision and Pattern Recognition, vol. 1, pp. 472–479. IEEE.

Neilson, J. D. and Geen, G. H. 1982. Otoliths of Chinook salmon (*Oncorhynchus tshawytscha*): daily growth increments and factors influencing their production. Canadian Journal of Fisheries and Aquatic Sciences, 39: 1340–1347.

Norderhaug, K., Christie, H., Fosså, J., and Fredriksen, S. 2005. Fish-macrofauna interactions in a kelp (*Laminaria hyperborea*) forest. Marine Biological Association of the United Kingdom. Journal of the Marine Biological Association of the United Kingdom, 85: 1279.

Norwegian Public Roads Administration 2017. *Thredds E39 - Breifjorden*. [online] Available at: http://thredds.met.no/thredds/catalog/obs/buoy-svv-e39/2017/06/catalog.html?dataset=obs/buoy-svv-e39/2017/06/201706_E39_D_Breisundet_wind.nc (Accessed: April 10th 2018).

Paine, R. T. 1966. Food web complexity and species diversity. The American Naturalist, 100: 65–75.

Pimm, S. L. and Lawton, J. 1977. Number of trophic levels in ecological communities. Nature, 268: 329–331.

Popper, A. N. and Fay, R. R. 1993. Sound detection and processing by fish: critical review and major research questions (part 1 of 2). Brain, behavior and evolution, 41: 14–25.

Preisendorfer, R. W. 1976. Hydrologic optics. volume 5. properties. Tech. rep., Honolulu: US Dept. of Commerce, National Oceanic and Atmospheric Administration, Environmental Research Laboratories, Pacific Marine Environmental Laboratory.

Quigley, M., Conley, K., Gerkey, B., Faust, J., Foote, T., Leibs, J., Wheeler, R., *et al.* 2009. ROS: an open-source Robot Operating System. *In* ICRA workshop on open source software, vol. 3, p. 5. Kobe, Japan.

Quintela, M., Danielsen, E. A., Lopez, L., Barreiro, R., Svåsand, T., Knutsen, H., Skiftesvik, A. B., *et al.* 2016. Is the ballan wrasse (*Labrus bergylta*) two species? Genetic analysis reveals within-species divergence associated with plain and spotted morphotype frequencies. Integrative zoology, 11: 162–172.

Rand, D., Lehman, B., and Shteynberg, A. 2007. Issues, models and solutions for triac modulated phase dimming of led lamps. *In* Power Electronics Specialists Conference, pp. 1398–1404. IEEE.

Ravanbakhsh, M., Shortis, M. R., Shafait, F., Mian, A., Harvey, E. S., and Seager, J. W. 2015. Automated fish detection in underwater images using shape-based level sets. The Photogrammetric Record, 30: 46–62.

Rice, J. 1995. Food web theory, marine food webs, and what climate change may do to northern marine fish populations. *In* Climate Change and Northern Fish Population, edited by R. J. Beamish, pp. 561–568. Publication of Fisheries and Aquatic Sciences, 121.

Rinde, E., Sloreid, S., Bakkestuen, V., Bekkby, T., Erikstad, L., and Longva, O. 2004. Modellering av utvalgte marine naturtyper og EUNIS klasser. To delprosjekter under det nasjonale programmet for kartlegging og overvåking av biologisk mangfold. NINA Oppdragsmelding, 807: 1–33. Norwegian Institute for Nature Research, Trondheim.

Ross, H. E., Franklin, S., Weltman, G., and Lennie, P. 1970. Adaptation of divers to size distortion under water. British Journal of Psychology, 61: 365–373.

Ross, R. M., Johnson, J. H., and Adams, C. M. 2005. Use of fish–otolith-length regressions to infer size of double-crested cormorant prey fish from recovered otoliths in lake ontario. Northeastern Naturalist, 12: 133–140.

Røv, N. 1984. Sjøfuglprosjektet 1979-1984. Norwegian Directorate for Nature Manangement, Viltrapport 35: 1–109.

Runde Miljøsenter 2018. *Om Runde*. [online] Available at: http://rundecentre.no/om-runde/ (Accessed: January 22nd 2018).

Ruxton, G. D., Sherratt, T. N., and Speed, M. P. 2004. Avoiding attack: the evolutionary ecology of crypsis, warning signals and mimicry. Oxford University Press, UK.

Ryther, J. H. 1969. Photosynthesis and fish production in the sea. Science, 166: 72–76.

Sakshaug, E., Johnsen, G., and Volent, Z. 2009. Light. *In* Ecosystem Barents Sea, edited by E. Sakshaug, G. Johnsen, and K. Kovavs, chap. 5, pp. 139–166. Tapir Academic Press, Trondheim.

Salvanes, A., Giske, J., and Nordeide, J. 1994. Life history approach to habitat shifts for coastal cod. Aquaculture and Fisheries Management, 25: 215–228.

Schjølberg, I. and Utne, I. B. 2015. Towards autonomy in ROV operations. IFAC-PapersOnLine, 48: 183–188.

Shannon, C. and Weaver, W. 1949. A mathematical model of communication. University of Illinois Press, USA.

Sigovini, M., Keppel, E., and Tagliapietra, D. 2016. Open nomenclature in the biodiversity era. Methods in Ecology and Evolution, 7: 1217–1225.

Skadsheim, A., Christie, H., and Leinaas, H. 1995. Population reductions of Strongylocentrotus droebachiensis (Echinodermata) in Norway and the distribution of its endoparasite *Echinomermella matsi* (Nematoda). Marine Ecology Progress Series, 119: 199–209.

Skiftesvik, A. B., Durif, C. M., Bjelland, R. M., and Browman, H. I. 2014. Distribution and habitat preferences of five species of wrasse (Family Labridae) in a Norwegian fjord. ICES Journal of Marine Science, 72: 890–899.

Smith, R. C. and Baker, K. S. 1981. Optical properties of the clearest natural waters (200–800 nm). Applied optics, 20: 177–184.

Spampinato, C., Giordano, D., Di Salvo, R., Chen-Burger, Y.-H. J., Fisher, R. B., and Nadarajan, G. 2010. Automatic fish classification for underwater species behavior understanding. *In* Proceedings of the first ACM international workshop on Analysis and retrieval of tracked events and motion in imagery streams, vol. 23, pp. 45–50. ACM digital Library.

Spellerberg, I. F. and Fedor, P. J. 2003. A tribute to claude shannon (1916–2001) and a plea for more rigorous use of species richness, species diversity and the 'shannon–wiener'index. Global ecology and biogeography, 12: 177–179.

Stelzenmüller, V., Breen, P., Stamford, T., Thomsen, F., Badalamenti, F., Borja, Á., Buhl-Mortensen, L., *et al.* 2013. Monitoring and evaluation of spatially managed areas: a generic framework for implementation of ecosystem based marine management and its application. Marine Policy, 37: 149–164.

Steneck, R. S., Graham, M. H., Bourque, B. J., Corbett, D., Erlandson, J. M., Estes, J. A., and Tegner, M. J. 2002. Kelp forest ecosystems: biodiversity, stability, resilience and future. Environmental conservation, 29: 436–459.

Stirling, G. and Wilsey, B. 2001. Empirical relationships between species richness, evenness, and proportional diversity. The American Naturalist, 158: 286–299.

Stoner, A. W., Ryer, C. H., Parker, S. J., Auster, P. J., and Wakefield, W. W. 2008. Evaluating the role of fish behavior in surveys conducted with underwater vehicles. Canadian Journal of Fisheries and Aquatic Sciences, 65: 1230–1243.

Telem, G. and Filin, S. 2010. Photogrammetric modeling of underwater environments. ISPRS Journal of Photogrammetry and Remote Sensing, 65: 433–444.

Teletchea, F., Laudet, V., and Hänni, C. 2006. Phylogeny of the Gadidae (sensu Svetovidov, 1948) based on their morphology and two mitochondrial genes. Molecular phylogenetics and evolution, 38: 189–199.

Thimijan, R. W. and Heins, R. D. 1983. Photometric, radiometric, and quantum light units of measure: a review of procedures for interconversion. HortScience, 18: 818–822.

Uglem, I., Rosenqvist, G., and Wasslavik, H. S. 2000. Phenotypic variation between dimorphic males in corkwing wrasse. Journal of fish biology, 57: 1–14.

United Nations 1992. United Nations Convention on Biological Diversity. [online] Available at: https://www.cbd.int/doc/legal/cbd-en.pdf, (Accessed: May 19th 2018).

Valiela, I. 1984. Marine ecological processes. Springer-Verlag, New York, 546 pp.

Vandenabeele, S. P., Grundy, E., Friswell, M. I., Grogan, A., Votier, S. C., and Wilson, R. P. 2014. Excess baggage for birds: inappropriate placement of tags on gannets changes flight patterns. PloS one, 9: e92657.

Vignon, M. and Morat, F. 2010. Environmental and genetic determinant of otolith shape revealed by a non-indigenous tropical fish. Marine Ecology Progress Series, 411: 231–241.

Villalba, L. J. G., Orozco, A. L. S., and Corripio, J. R. 2015. Smartphone image clustering. Expert Systems with Applications, 42: 1927–1940.

Villegas-Ríos, D., Alonso-Fernández, A., Fabeiro, M., Bañón, R., and Saborido-Rey, F. 2013. Demographic variation between colour patterns in a temperate protogynous hermaphrodite, the ballan wrasse *Labrus bergylta*. PloS one, 8: e71591.

Volent, Z., Johnsen, G., and Sigernes, F. 2007. Kelp forest mapping by use of airborne hyperspectral imager. Journal of Applied Remote Sensing, 1: 011503.

Walther, G.-R., Post, E., Convey, P., Menzel, A., Parmesan, C., Beebee, T. J., Fromentin, J.-M., *et al.* 2002. Ecological responses to recent climate change. Nature, 416: 389–395.

Weimerskirch, H. 2007. Are seabirds foraging for unpredictable resources? Deep Sea Research Part II: Topical Studies in Oceanography, 54: 211–223.

Weimerskirch, H., Cherel, Y., Cuenot-Chaillet, F., and Ridoux, V. 1997. Alternative foraging strategies and resource allocation by male and female wandering albatrosses. Ecology, 78: 2051–2063.

Weste, N. H. and Eshraghian, K. 1994. Principles of CMOS VLSI design: A systems perspective second edition. Addision-Wesley Publishing, California, USA.

WoRMS 2018. World Register of Marine Species (WoRMS). [online] Available at: http://www.marinespecies.org, (Accessed: January 11th 2018).

Yr.no 2018. *Detailed weather statistics for Runde*. [online] Available at: {https://www.yr.no/place/Norway/M%C3%B8re_og_Romsdal/Her%C3%B8y/Runde/detailed_statistics.html} (Accessed: 21st January 2018).

Yu, N., Genevet, P., Kats, M. A., Aieta, F., Tetienne, J.-P., Capasso, F., and Gaburro, Z. 2011. Light propagation with phase discontinuities: generalized laws of reflection and refraction. Science, 334: 333–337.

A Shannon diversity index calculation

Table A.1: An example from Transect #1 calculations of Shannon's Diversity Index derived from **Equation 2.6.1.1** and **Equation 2.5.2.2**; where H'_{max}, n = 1 for max diversity in every species.

Species	**Counted fish**	**P_i(n/sum(n))**	**P_i(log(P_i))**	**H'_{max}**	**E**
Cod (< 10 cm)	0			-0.09	
Cod (10-20 cm)	0			-0.09	
Cod (> 20 cm)	0			-0.09	
Saithe (< 10 cm)	12	0.26	-0.15	-0.09	
Saithe (10-20 cm)	0			-0.09	
Saithe (> 20 cm)	4	0.09	-0.09	-0.09	
Gadidae indet. (< 10 cm)	2	0.04	-0.06	-0.09	
Labridae indet. (< 10 cm)	8	0.17	-0.13	-0.09	
Goldsinny wrasse (< 10 cm)	0			-0.09	
Goldsinny wrasse (> 10 cm)	0			-0.09	
Corkwing wrasse (< 10 cm)	12	0.26	-0.15	-0.09	
Corkwing wrasse (> 10 cm)	0			-0.09	
Cuckoo wrasse (< 10 cm)	9	0.19	-0.14	-0.09	
Sum	**47**		**0.72**	**1.11**	**0.65**

B Back-calculation of fish length

Table B.1: The length of each species back-calculated from the length of otoliths found in Shag pellets. Lengths are calculated from equations given by Härkönen (1986) and Jobling and Breiby (1986).

	Length of fish (mm)				
Species	**Min**	**Mean**	**Max**	**SD**	**n**
Symphodus melops - Corkwing wrasse	123.77	**142.84**	180.96	9.83	8
Labrus mixtus - Cuckoo wrasse	214.14	**214.14**	214.14	-	1
Ctenolabrus rupestris - Goldsinny wrasse	98.09	**108.69**	123.64	8.86	10
Labridae indet. - Wrasse family	44.90	**80.96**	171.26	21.41	264
Gadidae indet. - Cod family	67.39	**116.23**	167.30	38.49	26
Gadus morhua - Cod	67.73	**151.08**	238.27	34.92	41
Pollachius pollachius - Pollack	103.23	**149.74**	181.96	19.29	24
Trisopterus minutus - Poor cod	20.33	**100.41**	216.96	27.11	249
Raniceps raninus - Tadpole fish	85.25	**85.25**	85.25	-	1
Ciliata spp. - Rockling	128.44	**164.04**	220.73	32.16	7
Pollachius virens - Saithe	21.62	**54.39**	304.04	27.44	590
Gobius niger - Black goby	146.61	**146.61**	146.61	-	1
Gobiidae - Gobies	11.93	**29.25**	59.84	15.59	13
Taurulus bubalis - Longspined bullhead	42.44	**73.22**	103.12	15.26	54
Pholis gunnellus - Rock gunnel	88.21	**101.26**	123.00	16.66	4
Ammodytes spp. - Sand lances	68.92	**99.03**	120.22	6.16	99
Zoarces viviparus - Viviparous eelpout	101.86	**112.62**	155.65	24.06	5